U.S. DEPARTMENT OF COMMERCE
NATIONAL OCEANIC AND ATMOSPHERIC ADMINISTRATION

U.S. DEPARTMENT OF THE ARMY
CORPS OF ENGINEERS

HYDROMETEOROLOGICAL REPORT NO. 49

Probable Maximum Precipitation Estimates, Colorado River and Great Basin Drainages

REPRINTED 1984

Prepared by
E. Marshall Hansen,
Francis K. Schwarz, and John T. Riedel
Hydrometeorological Branch
Office of Hydrology
National Weather Service

Silver Spring, Md.

For sale by the Superintendent of Documents, U.S. Government Printing Office
Washington, D.C. 20402

Stock No. 003-017-00408-2

ERRATA

Page

45, line 6: Change "summary" to "summer."

68, line 22: Add a closing parenthesis after "spreading out."

115, figure 4.5: Some latitude markings (ticks) on the 110th, 115th, and 120th meridians are incorrectly positioned; such markings should agree with those on the 105th and 125th meridians.

118, line 4: Change the period (.) to a colon (:) at the end of the line.

119, table 4.3, number 3: Change "1945" to "1943."

147, line 16: Change to read "figures 3.11a to d (Revised)."

148, step A.2,
149, step B.4,
152, title,
154, title: In computing the reduction for elevation for local-storm PMP, use mean basin elevation (mean elevation of area enclosed by basin boundary and limiting isohyet of storm pattern if areal distribution is used) instead of lowest (minimum) elevation in drainage. [In the example given on pages 154 and 155, if the mean elevation of 6500 ft had been used instead of the lowest (minimum) elevation, a somewhat reduced local storm PMP would have been computed.]

150, step B.1: Change to read "figures 3.11a to d (Revised)."

150, step B.5: Change to read "(table 3.9)."

151, line 2: Change to read "Area 878 mi^2."

151, line B.5: Change to read "(table 3.9)."

CONTENTS

		Page
Abstract		1
1.	Introduction	1
1.1.	Purpose of report	1
1.2.	Authorization	2
1.3.	Scope	2
1.4.	Definition of probable maximum precipitation	2
1.5.	Methods of this report	4
1.6.	Organization of report	4
2.	Convergence component of PMP	5
2.1.	Introduction	5
2.1.1.	Method of determining general-storm PMP	5
2.1.2.	Definition of convergence PMP	5
2.1.3.	General storm relation to local storm	5
2.1.4.	Convergence PMP for adjoining regions	6
2.1.5.	Summary of procedure	6
2.2.	Mid-month 1000-mb (100-kPa) convergence PMP maps, 24 hrs, 10 mi^2 (26 km^2)	7
2.2.1.	Envelopment of maximum observed rainfalls	7
2.2.2.	Enveloping 12-hr persisting dew points	11
2.2.3.	Regional patterns	11
2.2.4.	Seasonal variation	12
2.2.5.	PMP storm prototypes	18
2.2.6.	Development of 10-mi^2 (26-km^2) 24-hr convergence PMP	19
2.3.	Effect of barrier and elevation	34
2.3.1.	Effective barrier and elevation map	34
2.3.2.	Reduction for effective barrier and elevation	34
2.4.	Depth-duration variation	36
2.4.1.	Data	36
2.4.2.	Depth-duration relation	39
2.4.3.	Seasonal variation	41
2.4.4.	Regional variation	45
2.5.	Areal reduction for basin size	50
3.	Orographic component of PMP	53
3.1.	Introduction	53
3.1.1.	Methods for determining orographic effects on rainfall	53
3.1.2.	Definition of orographic precipitation	53
3.1.3.	Detail in orographic PMP	55
3.2.	Orographic index map	56
3.2.1.	Development of first approximation	57
3.2.2.	Guidance to modification	58
3.2.2.1.	Rain ratios for line segments	58
3.2.2.2.	Rain ratios for central Arizona	62
3.2.2.3.	Effects to lee of ridges	63
3.2.2.4.	Summary	65

Page

3.2.3. Modifications to index map. 67
3.2.3.1. In areas of most-orographic effects 67
3.2.3.2. In areas of least-orographic effects. 68
3.2.3.3. In areas of intermediate-orographic effects 68
3.2.3.4. Other modifications 69
3.2.4. Modified orographic PMP index map 69
3.3. Seasonal variation. 69
3.3.1. Introduction. 69
3.3.2. Boundary regions. 70
3.3.3. Indices within the region 79
3.3.3.1. Maximum precipitation at high elevations. 79
3.3.3.2. Maximum winds and moisture. 79
3.3.3.3. Orographic model computations 79
3.3.4. Smoothed maps 80
3.3.5. Supporting evidence 80
3.4. Variation with basin size 88
3.4.1. Introduction. 88
3.4.2. Storm data. 90
3.4.3. Adopted variation 92
3.5. Durational variation. 92
3.5.1. Background. 92
3.5.2. Variation of maximum winds. 93
3.5.3. Variation of maximum moisture 94
3.5.4. Variation of relative humidity. 95
3.5.5. Orographic model computation. 95
3.5.6. Guidance from observed precipitation. 97
3.5.7. Adopted variation 99
4. Local-storm PMP for the Southwestern Region and California. 103
4.1. Introduction. 103
4.1.1. Region of interest. 103
4.1.2. Definition of local storm 105
4.2. Storm record. 105
4.3. Development of 1-hr PMP 108
4.3.1. Introduction. 108
4.3.2. Data adjustments. 109
4.3.2.1. Application of adjustments to data. 111
4.3.3. Analysis. 111
4.4. Durational variation. 116
4.4.1. Duration of local-storm PMP 116
4.4.2. Data and analysis for durations from 1 to 6 hours . . . 116
4.4.3. Data and analysis for less than 1-hr duration 119
4.5. Depth-area relation 120
4.6. Distribution of PMP within a basin. 122
4.7. Time distribution of incremental PMP. 122
4.8. Seasonal distribution 127
5. Checks on the general level of PMP. 129
5.1. Introduction. 129
5.2. Comparisons with greatest known general-storm areal rainfalls 129

Page

5.3. Comparisons with greatest known local-storm rainfalls. . . 133
5.4. Comparisons with estimates from a previous study 135
5.5. Comparisons with 100-yr return period rainfalls 135
5.6. Mapped ratios of 100-yr to PMP values over the Western States 137
5.7. An alternate approach to PMP 139
5.8. Statistical estimates of PMP 140
5.8.1. Background 140
5.8.2. Computations 141
5.8.3. Discussion 141
5.9. Hypothesized severe tropical cyclone 142
5.9.1. Transposition and adjustment of PMP based on the Yankeetown, Fla. storm of September 5-6, 1950. 143
5.10. Conclusion on PMP checks 145
6. Procedures for computing PMP 146
6.1. Introduction 146
6.2. Steps for computing general-storm PMP for a drainage . . . 146
6.3. Steps for computing local-storm PMP. 148
Acknowledgements 156
References 157

TABLES

2.1. Most extreme general-storm convergence rainfalls 9

2.2. Stations within least-orographic regions for which daily precipitation was available for 20 years or more before 1970 13

2.3. Seasonal variations of 1000-mb (100-kPa) convergence PMP for 24 hours, from HMR No. 43 (USWB 1966a) 18

2.4. Stations within least-orographic regions for which hourly precipitation data were available for the period 1948 through 1972. 38

2.5. Nonsummer storms in the Southwest and the number of stations with relatively large rainfalls in least-orographic regions used in duration analysis of convergence PMP 39

2.6 Comparison of 6/24-hr ratios in the Northwest and Southwest studies at 42°N, 113°W 46

2.7. Durational variation of convergence PMP. 50

3.1. Summary of average rain ratios. 61

3.2. Average rain ratio for 9 selected upslope segments in Arizona (B, D, E, F, G, H, I, J, K in fig. 4.5). 61

3.3. Seasonal variation east of Cascade Ridge in Northwest States as percent of August 70

Page

3.4. Seasonal variation in Pacific drainage of California as percent of August. 70

3.5. Data analyzed for determining depth-area variation of orographic PMP 91

3.6. Durational variation of maximum moisture of the Southwest 94

3.7. Computation of durational variation of orographic precipitation for the Southwest States using a simplified orographic model. 98

3.8. Durational variation in major storms in orographic locations; Southern California and Arizona. 100

3.9. Durational variation of orographic PMP 103

4.1. Major short-period rains of record in the Southwestern States and all of California 106

4.2. Adjustment to most critical local-storm rainfalls. . . . 113

4.3. Depth-duration relations of severe local storms. 119

4.4. Durational variation of 1-mi^2 (2.6-km^2) local-storm PMP in percent of 1-hr PMP. 120

4.5. Isohyetal labels for the 4 highest 15-min PMP increments and for 1-hr PMP 124

4.6. Isohyetal labels for second to sixth hourly incremental PMP in percent of 1-hr 1-mi^2 (2.6-km^2) PMP 125

4.7. Time sequence for hourly incremental PMP in 6-hr storm . 126

4.8. Time sequence for 15-min incremental PMP within 1 hr . . 127

4.9. Seasonal distribution of thunderstorm rainfalls. 127

5.1. Comparison of storm areal rainfall depths with general-storm PMP for the month of the storm 130

5.2. Adjustment of tropical storm PMP for distance-from-coast 145

6.1. General-storm PMP computations for the Colorado River and Great Basin. 150

6.2. Example computation of general-storm PMP 151

6.3. Local-storm PMP computations, Colorado River, Great Basin and California drainages 152

Page

6.4. Example computations of local storm PMP. 154

FIGURES

1.1. Primary study area, Colorado River and Great Basin Drainages. 3

2.1. Location of stations used in studies of 1- and 3-day rainfall 8

2.2. Location of most extreme general-storm convergence rainfalls in the Southwest. 10

2.3. Examples of schematic diagrams depicting moisture sources (arrows) implied by gradients of 12-hr persisting 1000-mb (100-kPa) dew points, January and August. 14

2.4. Seasonal variation of convergence PMP and supporting data for least-orographic subregions; a. Southwest Arizona, b. northeast Arizona. 15

2.4. Seasonal variation of convergence PMP and supporting data for least-orographic subregions; c. western Utah, d. southern Nevada. 16

2.4. Seasonal variation of convergence PMP and supporting data for least-orographic subregions; e. northwest Nevada. . . . 17

2.5. 1000-mb (100-kPa) 24-hr convergence PMP (inches) for 10 mi^2 (26 km^2) for January. 22

2.6. 1000-mb (100-kPa) 24-hr convergence PMP (inches) for 10 mi^2 (26 km^2) for February 23

2.7. 1000-mb (100-kPa) 24-hr convergence PMP (inches) for 10 mi^2 (26 km^2) for March. 24

2.8. 1000-mb (100-kPa) 24-hr convergence PMP (inches) for 10 mi^2 (26 km^2) for April. 25

2.9. 1000-mb (100-kPa) 24-hr convergence PMP (inches) for 10 mi^2 (26 km^2) for May. 26

2.10. 1000-mb (100-kPa) 24-hr convergence PMP (inches) for 10 mi^2 (26 km^2) for June 27

2.11. 1000-mb (100-kPa) 24-hr convergence PMP (inches) for 10 mi^2 (26 km^2) for July 28

2.12. 1000-mb (100-kPa) 24-hr convergence PMP (inches) for 10 mi^2 (26 km^2) for August 29

Page

2.13. 1000-mb (100-kPa) 24-hr convergence PMP (inches) for 10 mi^2 (26 km^2) for September. 30

2.14. 1000-mb (100-kPa) 24-hr convergence PMP (inches) for 10 mi^2 (26 km^2) for October. 31

2.15. 1000-mb (100-kPa) 24-hr convergence PMP (inches) for 10 mi^2 (26 km^2) for November 32

2.16. 1000-mb (100-kPa) 24-hr convergence PMP (inches) for 10 mi^2 (26 km^2) for December 33

2.17. Effective barrier and elevation heights (1000's of feet) for Southwestern States 35

2.18. Percent of 1000-mb (100-kPa) convergence PMP resulting from effective elevation and barrier considerations. 37

2.19. Relation between 6/24-hr and 72/24-hr ratios for within-storm cases of 3 consecutive day rainfall for all stations listed in table 2.4. 40

2.20. Idealized depth-duration curves in percent of 24-hr amount. . 42

2.21. Adopted 6/24-hr vs. 72/24-hr convergence PMP ratios 43

2.22. Seasonal variation of 6/24-hr ratios at least-orographic subregion midpoints. 44

2.23. Seasonal variation of 6/24-hr durational rainfall ratios for Southwest and adjacent regions. 44

2.24. Smoothed variation of 6/24-hr ratios at subregional midpoints 45

2.25. Regional variation of 6/24-hr ratios by month (percent); January to April 47

2.26. Regional variation of 6/24-hr ratios by month (percent); May to August 48

2.27. Regional variation of 6/24-hr ratios by month (percent); September to December 49

2.28 Depth-area variation for convergence PMP for first to fourth 6-hr increments; January to July. 51

2.29. Depth-area variation for convergence PMP for first to fourth 6-hr increments; August to December 52

Page

3.1. Areas of minimum orographic effects in Southwest States. . . 54

3.2. Schematic of orographic PMP index map development. 56

3.3. A first approximation to the orographic PMP (inches) for 10 mi^2 (26 km^2) 24 hr in southeast Arizona 57

3.4. Segments across major ridges in Southwest States used in rain ratio study 59

3.5. Segments across major ridges in Arizona superimposed on analysis of 100-yr 24-hr precipitation (in tenths of an inch) 60

3.6. Generalized topography and station locator map in vicinity of Workman Creek, Arizona. 62

3.7. Rainfall-elevation relation for August 1951 storm, and rainfall for September 1970 storm. 63

3.8. Leeward isohyetal patterns; a. 100-yr 24-hr rainfall, b. August 1951 storm 64

3.8. Leeward isohyetal patterns; c. September 1970 storm. 65

3.9. Leeward rainfalls in percent of ridge value for major storms and 100-yr 24-hr rains 66

3.10. Example of profiles of several rainfall indices (in percent of maximum values) 67

3.11a. 10-mi^2 (26-km^2) 24-hr orographic PMP index map (inches), northern section 71

3.11b. 10-mi^2 (26-km^2) 24-hr orographic PMP index map (inches), north-central section. 73

3.11c. 10-mi^2 (26-km^2) 24-hr orographic PMP index map (inches), south-central section. 75

3.11d. 10-mi^2 (26-km^2) 24-hr orographic PMP index map (inches), southern section 77

3.12. Seasonal variation in 10-mi^2 (26-km^2) 24-hr orographic PMP for the study region (in percent of values in figure 3.11); January, February. 81

3.13. Seasonal variation in 10-mi^2 (26-km^2) 24-hr orographic PMP for the study region (in percent of values in figure 3.11); March, April 82

Page

3.14. Seasonal variation in 10-mi^2 (26-km^2) 24-hr orographic PMP for the study region (in percent of values in figure 3.11); May, June 83

3.15. Seasonal variation in 10-mi^2 (26-km^2) 24-hr orographic PMP for the study region (in percent of values in figure 3.11); July, August. 84

3.16. Seasonal variation in 10-mi^2 (26-km^2) 24-hr orographic PMP for the study region (in percent of values in figure 3.11); September, October. 85

3.17. Seasonal variation in 10-mi^2 (26-km^2) 24-hr orographic PMP for the study region (in percent of values in figure 3.11); November, December. 86

3.18. Months of maximum total general-storm PMP for Southwest States, 10 mi^2 (26 km^2) 24 hr 87

3.19. Season and month of maximum and secondary maximum 24-hr station precipitation, after Pyke (1972). 87

3.20. Variation of orographic PMP with basin size 89

3.21. 1000-mi^2 (2590-km^2) storm depths relative to 10-mi^2 (26-km^2) depths for 72-hr rainfalls 90

3.22. Durational variation of maximum winds at Tucson, Arizona compared with variations for adjoining regions. 93

3.23. Durational variation of precipitable water. 95

3.24. Adopted durational variation in relative humidity and supporting data 96

3.25. Durational variation in orographic precipitation near northern and southern borders of Southwest region (from orographic model). 97

3.26. Ratios of 72/24-hr rains at high elevations from major storms in southern California and Arizona. 102

3.27. Adopted durational variation in orographic PMP. 102

4.1. Location of short-duration extreme rainfalls. 104

4.2. Variation of maximum 6-hr summer recorder rainfall with elevation (period of record is 1940-1972) 110

4.3. Variable depth-duration curves for 6-hr PMP in the Southwest States and all of California. 112

Page

4.4. Maximum clock-hour rainfalls at stations with records for period 1940-1972. 114

4.5. Local-storm PMP for 1 mi^2 (2.6 km^2) 1 hr. 115

4.6. Criteria of clock-hour rainfall amounts used for selection of storms at recorder stations for depth-duration analysis. 117

4.7. Analysis of 6/1-hr ratios of averaged maximum station data (plotted at midpoints of 2° latitude-longitude grid) . 119

4.8. Depth-area relations adopted for local-storm PMP in the Southwest and other data. 121

4.9. Adopted depth-area relations for local-storm PMP. 123

4.10. Idealized local-storm isohyetal pattern 126

4.11. Regional variation of month of maximum local-storm rainfall . 128

5.1. Comparison between observed rainfall depths and general-storm PMP for 100 mi^2 (259 km^2) 24 hr 133

5.2. Comparison between observed rainfall depths and general-storm PMP for 5000 mi^2 (12,950 km^2) 24 hr 134

5.3. Comparison between observed rainfall depths from local storms and local-storm PMP for the duration of the storm. . 134

5.4. General-storm PMP for 10 mi^2 (26 km^2) 24 hr in inches (upper number) and local-storm PMP for 10 mi^2 (26 km^2) 6 hr in inches (lower number) at 1° grid points. 136

5.5. Comparison between PMP from Technical Paper No. 38 (U.S. Weather Bureau 1960) and from this study. 136

5.6. Comparison between 100-yr rainfall (Miller et al. 1973) and PMP 137

5.7. Ratios of 100-yr point rainfall (Miller et al. 1973) to highest PMP for 10 mi^2 (26 km^2) 24 hr 138

5.8. Ratios of PMP determined from an alternate approach (see section 5.7) to that of this study for 10 mi^2 (26 km^2) 24 hr 140

Page

5.9. Comparison between statistical PMP (Hershfield 1965) and the highest PMP for 10 mi^2 (26 km^2) 24 hr at stations with records exceeding 50 years. 141

5.10. Distance-from-coast reduced tropical storm nonorographic PMP compared with 1000-mb (100-kPa) convergence PMP for August, 10 mi^2 (26 km^2) 24 hr. 144

PROBABLE MAXIMUM PRECIPITATION ESTIMATES, COLORADO RIVER AND GREAT BASIN DRAINAGES

E. Marshall Hansen, Francis K. Schwarz, and John T. Riedel
Hydrometeorological Branch
Office of Hydrology
NOAA, National Weather Service, Silver Spring, Md.

ABSTRACT. This study gives general-storm probable maximum precipitation (PMP) estimates for durations between 6 and 72 hours and for area sizes between 10 and 5,000 mi^2 (26 and 12,950 km^2), for any location in the Colorado River and Great Basin drainages. Total PMP is determined as the sum of convergence and orographic PMP components. Estimates are given for each month.

The study also provides estimates for local-storm PMP. In addition to the above drainages these estimates are provided for all of California. The estimates cover durations between 15 minutes and 6 hours and drainage areas between 1 and 500 mi^2 (2.6 and 1,295 km^2). Local-storm PMP is applicable to the warm season between May and October.

Comparisons are given between PMP estimates and the greatest observed rainfalls of record, 100-yr frequency rainfall and statistically derived PMP. A step-by-step outline of the procedure for computing PMP estimates is presented with examples for both the general and local storm.

1. INTRODUCTION

1.1 Purpose of Report

The purpose of this report is to present the material necessary to compute estimates of probable maximum precipitation for any watershed up to 5,000 mi^2 (12,950 km^2) for durations up to 72 hours in the Colorado River or Great Basin drainages. The material for preparing an estimate makes up only a small portion of this text; the bulk of the report consists of data and studies required to develop the criteria. The local-storm criteria presented in this report also cover the Pacific Ocean drainage of California.

1.2 Authorization

Authorization for the study was given in a memorandum from the Office of Chief of Engineers, Corps of Engineers, dated July 8, 1971. In conferences between representatives of the Corps of Engineers and the National Weather Service it was agreed the study should cover the Colorado River drainage and interior drainages of Nevada, Utah, and California. As thunderstorm PMP had not been previously considered for the Pacific Ocean drainages in California, it was subsequently agreed to expand this portion of the study.

1.3 Scope

Estimates of general-storm probable maximum precipitation (PMP) in this report cover the region between the crest of the Sierra Nevadas on the west and the Continental Divide on the east. To the north, the region extends to the southern limits of the Columbia River drainage and to the south to the U. S. border. This study region is shown in figure 1.1.

The shaded portion of the study region in figure 1.1 is a zone (to the west of the Continental Divide) where the PMP values are considered least certain. Detailed generalized PMP estimates including seasonal variation are not available for the slopes immediately east of the Continental Divide. PMP gradients in this region can influence PMP estimates west of the Divide. A future PMP study covering the area east of the Divide is needed before there will be comparable confidence in PMP over the contiguous portion of the Southwestern States.

General-storm PMP estimates may be obtained for basin sizes from 10 to 5,000 mi^2 (26 to 12,950 km^2) for durations from 6 to 72 hours. Values can be computed for each month.

Intense local summer thunderstorms can produce rain for short durations over small basins that exceed the rain potential from general storms. Chapter 4 gives these criteria for durations from 15 minutes to 6 hours covering basin sizes up to 500 mi^2 (1,295 km^2). The thunderstorm PMP estimates cover not only the primary study region defined above but also the remainder of California except a small section of the northern coastal region.

The meteorological background and discussions have been kept to a minimum. A companion report (Schwarz and Hansen 1978) contains detailed descriptions of the meteorology of storms and other major meteorological analyses.

1.4 Definition of Probable Maximum Precipitation

Probable maximum precipitation (PMP) is defined (American Meteorological Society 1959) as "...the theoretically greatest depth of precipitation for a given duration that is physically possible over a particular drainage basin at a particular time of year." We recognize there are yet unknowns in the complicated atmospheric processes responsible for extreme rainfalls. Thus, methods used for deriving PMP include making judgments based on record storms and meteorological processes related to them. Results of studies are considered estimates because changes are likely as our understanding increases.

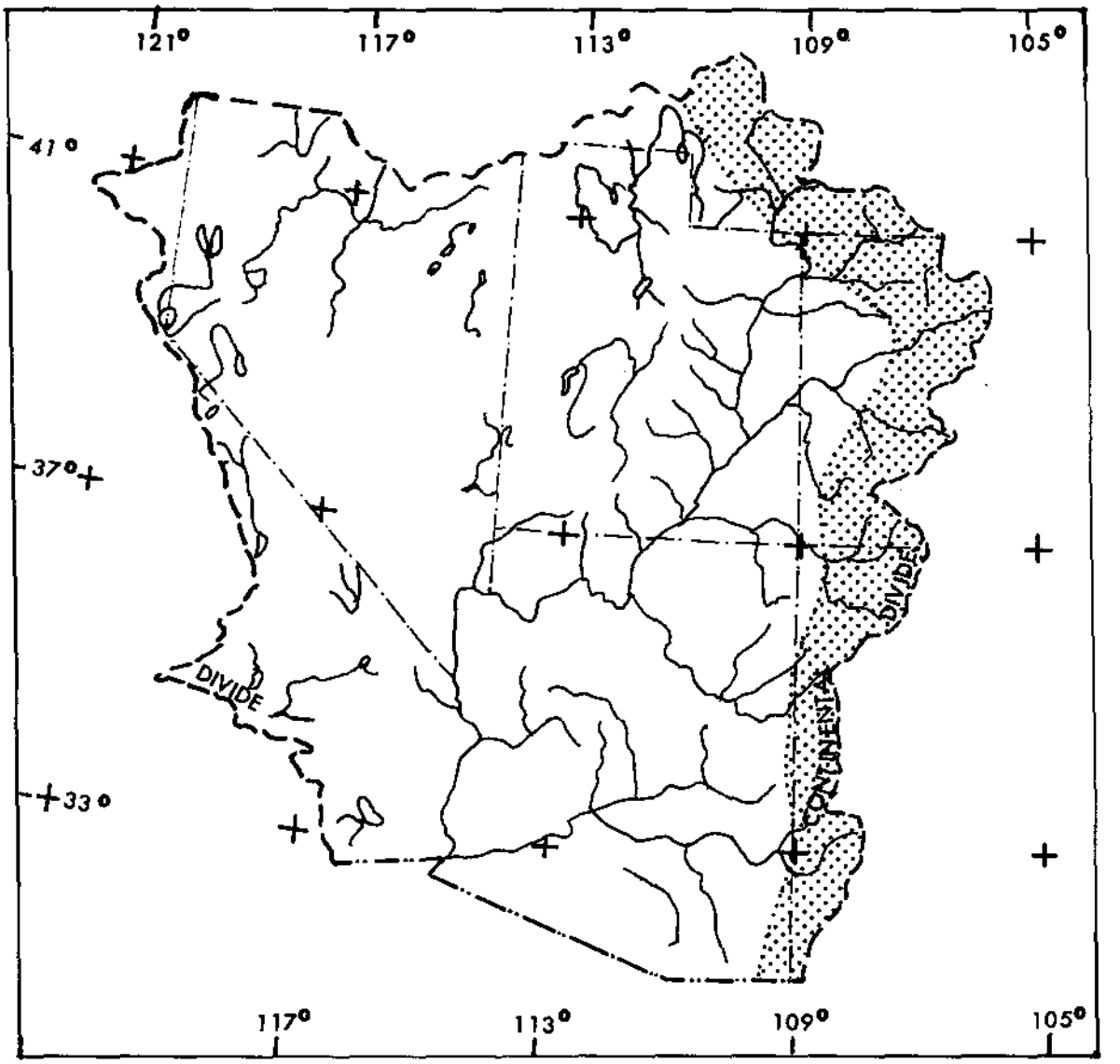

Figure 1.1.--Primary study area, Colorado River and Great Basin drainages. Criteria for shaded portion are considered of lesser reliability.

In this derivation of PMP we assume that the record storms during the past 80 or so years are representative of the climate of extreme precipitation. PMP estimates therefore do not allow for changes in climate.

Experience gained from PMP studies in other regions gives additional guidance to procedures and methods used. This then points to an operational definition of PMP; i.e., estimates by hydrometeorologists of upper limits of rainfall, supplied to engineers for use in hydrologic design. Quoting from Operational Hydrology Report No. 1 (World Meteorological Organization 1973), "Whatever the philosophical objection to the concept, the operational definition leads to answers that have been examined thoroughly by competent meteorologists and engineers and judged as meeting the requirements of a design criterion."

1.5 Methods of This Report

Estimation of general storm PMP of this report uses basically the same procedure used in two studies for adjoining regions; to the west (U. S. Weather Bureau 1961) and to the north (U. S. Weather Bureau 1966a). First, essentially nonorographic PMP, also termed convergence PMP (precipitation due to atmospheric processes), is estimated. Then orographic PMP (precipitation from moist air forced upward by mountain slopes and the triggering of rainfall near first upslopes) is estimated. The two components of PMP are then added together. The convergence PMP is based on moisture-maximized rains of record, reduced for mountain barriers and elevations. Consideration was given to convergence PMP from the adjoining studies. Orographic PMP, for the most part, was not based on the orographic precipitation computation model used in adjoining regions (U. S. Weather Bureau 1961 and 1966a). Reasons for this departure are spelled out in chapter 3. The model is not suited for the meteorological conditions accompanying the main PMP storm prototype for much of the Southwest, partly because the topography is too complicated. Alternate methods for estimating orographic PMP are discussed in chapter 3.

The method used for local or thunderstorm PMP was to adjust the most intense storm values for maximum moisture and develop a 1-hr PMP map for 1 mi^2 (2.6 km^2). The regional pattern of this map took into account maximum 1-hr rainfalls from recorder stations and broad-scale terrain features. Depth-duration and depth-areal variations to extend the estimates to other durations and larger areas were based on record storms.

1.6 Organization of Report

General-storm convergence PMP estimates are developed in chapter 2 and general storm orographic PMP in chapter 3. PMP for small areas from intense thunderstorms is covered in chapter 4. Checks on the general level of PMP are discussed in chapter 5; while chapter 6 gives procedures for and examples of use of the developed criteria.

We at times refer to the study region as the Southwest or the Southwestern States. Frequent reference will be made to studies for two adjoining regions. These are the Columbia River drainage, Hydrometeorological Report No. 43 (U. S. Weather Bureau 1966a) and the Pacific Ocean drainages of

California, Hydrometeorological Report No. 36 (U.S. Weather Bureau 1961). Hereafter they will be referred to as HMR No. 43 and HMR No. 36, respectively.

2. CONVERGENCE COMPONENT OF PMP

2.1 Introduction

2.1.1 Method of Determining General-Storm PMP

We noted in chapter 1 that the method for determining general-storm PMP in this study was to make separate estimates of orographic and nonorographic PMP; to judge the regional, seasonal, depth-area, and depth-duration variations of each component; and then to add the components for an estimate of total PMP. This method is comparable to that used for general-storm PMP estimates to the west and north (HMR No. 36 and No. 43). Development of nonorographic PMP, or convergence PMP, is the subject of this chapter.

2.1.2 Definition of Convergence PMP

Nonorographic precipitation can be defined as precipitation resulting from atmospheric processes not affected by terrain. Lifting and therefore cooling of moist air are necessary for major precipitation. Lifting or vertical motion can be produced by horizontal convergence of air at lower levels; hence, the term "convergence" for nonorographic precipitation. Under this definition all precipitation in regions with no abrupt changes in elevation is classified as convergence. Convergence and orographic precipitation can occur simultaneously.

2.1.3 General Storm Relation to Local Storm

In the United States east of approximately the 105th meridian, many extreme small area rainfalls have occurred within longer storm periods in which general rains cover larger areas. In contrast, experience has shown that the greatest short-duration rainfalls over small areas in the intermountain region come from intense local storms (thunderstorms) as opposed to general-storm situations. For the Southwestern States, therefore, separate estimates of local-storm PMP are given in chapter 4. While most extreme point rainfalls of record in the Southwest States have been isolated with regard to space and time, this does not negate the occurrence of lesser thunderstorm rains imbedded in the general PMP storm prototype. The point to be emphasized is that the local thunderstorm, the greatest potential rainfall threat for small areas and short durations, is an isolated event in time and space in the Southwestern States, while less intense thunderstorm occurring within general-storm rains are the key for general-storm convergence PMP.

2.1.4 Convergence PMP for Adjoining Regions

The Southwest States Region is bounded on the west by the Pacific Ocean drainage of California. Convergence PMP estimates for that drainage (HMR No. 36) were based on multiplying greatest observed ratios of P/M_s by M_x (observed precipitation, P, divided by storm moisture, M_s, multiplied by maximum moisture, M_x). The P/M_s ratios were associated with rains at least-orographic locations such as on the floor of the Central Valley of California. Enveloping values of P/M_s and a regional pattern of M_x were used to determine a basic convergence PMP index map for 10 mi^2 (26 km^2) for 6 hours duration.

For the Columbia River drainage to the north (HMR No. 43), similar procedures for estimating convergence PMP were used. The major difference from HMR No. 36 was that regional patterns of convergence PMP were determined for each month, October through June. These monthly maps incorporated the seasonal variations of maximum observed 1-day precipitation at groups of least-orographic stations as well as the seasonal variation of maximum moisture.

In developing convergence PMP for the present study, reasonable consistency was maintained with values for the two adjoining regions.

Also of some interest are PMP estimates for the United States east of the 105th meridian (Schreiner and Riedel 1978, and Riedel et al. 1956). For these studies, the effects of steepening slopes near the 105th meridian in Colorado and New Mexico were not taken into account. Thus, the PMP estimates to the east of the steep slopes of the Rocky Mountains should be considered nonorographic. The steep slopes east of the Continental Divide separate by distances up to 300 miles (483 km), the region of those studies from that of the present study. Sharp gradients in precipitation potential are expected in this intervening region that do not allow detailed comparisons of PMP between the two studies. Some overall general consistency checks can be made, such as the effect of moisture sources on PMP patterns, etc. Checks of this nature have been considered in this study.

2.1.5 Summary of Procedure

The approach for convergence PMP in this study follows after but is not identical with that for HMR Nos. 36 and 43. Instead of developing P/M_s ratio envelopes, the greatest moisture-maximized observed rainfalls for least-orographic locations were enveloped. This is equivalent to the previous studies [(P/M_s) envelope x M_x = $(P \times M_x/M_s)$ envelope]. Monthly patterns of highest moisture and seasonal trends in maximum observed precipitation were used as guides in interpolating between locations of highest moisture-maximized rainfalls. The resulting patterns are consistent with patterns of convergence PMP in HMR No. 43 and No. 36. The 1000-mb (100-kPa) convergence PMP estimates were then reduced for effective elevation and barrier. Depth-duration (from 6 to 72 hours) and depth-area (from 10 to 5,000 mi^2, 26 to 12,950 km^2) relations were based on maximum observed precipitation in least-orographic areas of the Southwestern States and those from eastern states data respectively. These procedures are in general agreement with those used in HMR No. 36 and HMR No. 43.

2.2 Mid-Month 1000-mb (100-kPa) Convergence PMP Maps, 24 hrs, 10 mi^2 (26 km^2)

2.2.1 Envelopment of Maximum Observed Rainfalls

Record storm rainfall is the underpinning to any PMP study. We need two restrictions to our data sample. First, extreme isolated thunderstorm values are not appropriate for development of general-storm convergence PMP. Such values rather are the basis for the local-storm PMP estimates of chapter 4. Secondly, in this section we are concerned with only the convergence component of record storm amounts. No consistent method has been found for separating total observed storm precipitation into convergence and orographic components; however, we can restrict the data to observed maxima in least-orographic regions of the Southwest.

Least-orographic regions are subjectively determined zones (shown in fig. 2.1) outlined on a 1:2,000,000 scale topographic map. The boundary of each subregion depicted on the figure is not significant other than to enclose a group of at least five stations whose precipitation we believe to be least influenced by orography. An appreciation for the complex terrain and an aid in determining general limits for these subregions was gained by two of the authors (Riedel and Hansen) during a 2-day series of overflights in 1972. We recognize that some substantial orographic features remain within the least-orographic boundaries shown in figure 2.1 but stations selected within these subregions were judged not to be significantly influenced by orography. An attempt was made to obtain an equal number of stations in each subregion, but this was difficult to maintain. Station storm totals exceeding 5 inches (127 mm) in 24 hours or less in the subregions were extracted from the historical records. The five storms meeting this criterion are listed in table 2.1. One other storm for Porter, N.M., east of the region of interest, is listed for comparison. Meteorological descriptions of each of the events is given in the companion report (Schwarz and Hansen 1978). Each storm total is the result of thunderstorms sustained over a period of 6 hours or more within a more general precipitation storm. This distinguishes them from the isolated thunderstorm events used for local-storm PMP.

The locations of storms listed in table 2.1 are shown in figure 2.2. San Luis, Mexico lies just south of the study region. Since the exact duration of the San Luis 1-day storm amount (Secretaria de Recursos Hydrolicos 1970) could not be determined, a duration of 24 hours was used.

Two of the 5 values in table 2.1, at Bug Pt., Utah and Dove Ck. 10 SW, Colo., occurred in the September 4-6, 1970 storm. These stations near the edge of an outlined least-orographic region (see fig. 2.1) reported rainfalls of 6.50 inches (165 mm) and 6.00 inches (152 mm), respectively. They are on a high plateau at elevations of 6600 and 6900 feet (2012 and 2103 m) respectively. Analysis of orographic PMP in the following chapter shows that some minimum-orographic effect is necessary over this subregion. Analyses of other notable general storms for the region (i.e. the September 4-7 and 11-13, 1939 and August 28-30, 1951 Arizona storms), disclosed that maximum precipitation for these storms occurred primarily in orographic regions. Total storm amounts were all less than 3 inches (76 mm) at least-orographic stations.

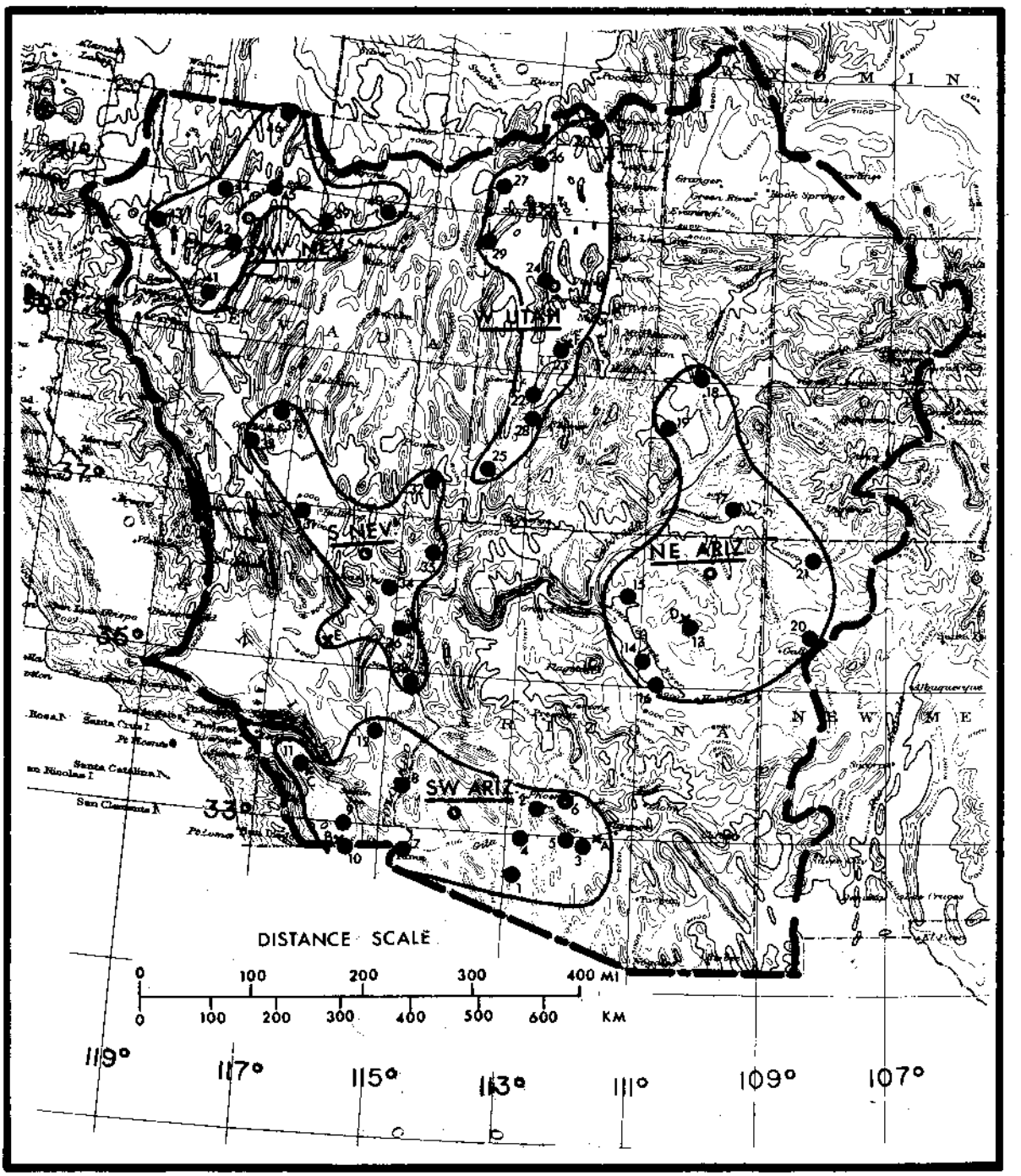

Figure 2.1.--Location of stations used in studies of 1- and 3-day rainfall. Numbered stations listed in table 2.2. Letters by X-stations refer to additional stations listed in table 2.4. Least-orographic regions considered for grouping stations into subregions enclosed by solid lines. Double circles indicate approximate midpoints for each subregion discussed in section 2.2.1.

Table 2.1.--Most extreme general-storm convergence rainfalls

Storm location	Date	Amount in.	Amount (mm)	Duration hr	Elevation ft	Elevation (m)	Elev. Adj.	Dura. Adj.	Moist Adj.	Adj. Storm Amt. in.	Adj. Storm Amt. (mm)
Indio, Calif. (33°43, 116°14)	9-24-39	6.45	(164)	6	20	(6)	100	141	134	12.2	(310)
Casa Grande Ruins, Ariz. (33°00, 111°33)	8-1-06	5.4	(137)	6.5	1400	(427)	113	128	116	9.1	(231)
San Luis, Sonora, Mex. (32°30, 114°48)	11-26-67	7.64	(194)	24*	0	(0)	100	100	120	9.2	(234)
Dove Ck.10SW,Colo. (37°45, 108°55)	9-5-70	6.00[Δ]	(152)	12	6900	(2103)	208	115	111	15.9	(404)
Bug Pt., Utah (37°38, 109°05)	9-5-70	6.50[Δ]	(165)	12	6600	(2012)	200	115	111	16.6	(422)
Porter, N. M. (35°13, 103°17)	10-10-30	9.91	(252)	24	4100	(1250)	152	100	148	22.3	(566)

*Duration has not been verified.

[Δ]Has some orographic contamination.

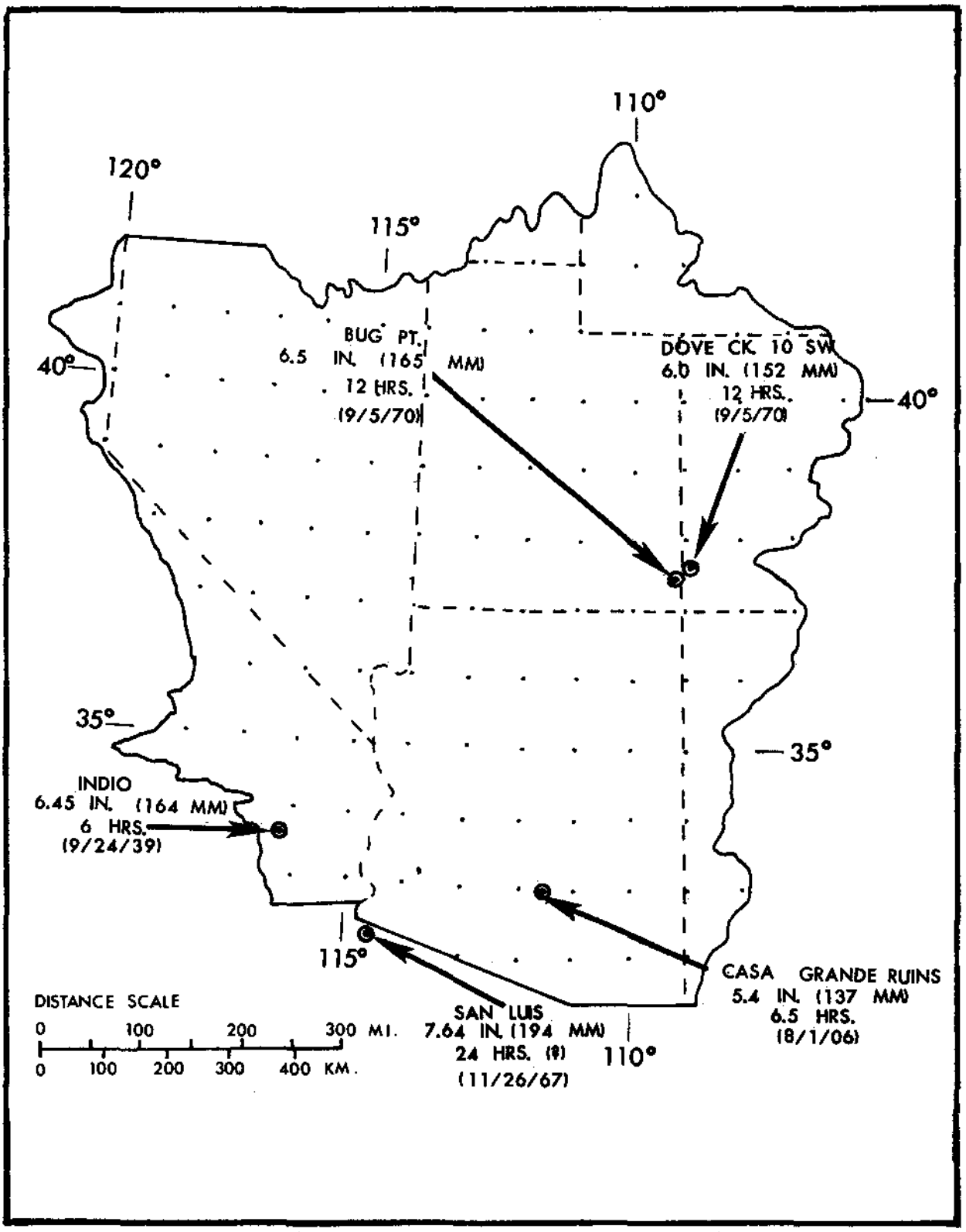

Figure 2.2.--Location of most extreme general-storm convergence rainfalls in the Southwest.

The major nonsummer general storms such as February 3-8, 1937, November 25-28, 1905 and December 14-17, 1908, also indicated less than 3 inch (76 mm) total storm amounts for least-orographic stations. Taken collectively, and excluding the Porter storm, the amounts listed in table 2.1 are the greatest known general-storm convergence point rainfalls for the Southwest.

The storm values were adjusted to a common elevation and duration, and to optimum moisture conditions. The adjustments are as follows:

a. Adjustment for elevation. The events of table 2.1 were adjusted to sea level (assumed 1000 mb, 100 kPa). This adjustment is the ratio of the available precipitable water above 1000 mb (100 kPa) to that available above the surface. Where adjustments were necessary, the precipitable water was determined using the storm 12-hr persisting 1000-mb (100-kPa) dew point and assuming a pseudo-adiabatic saturated atmosphere (U. S. Weather Bureau 1951a).

b. Adjustment for duration. A generalized durational variation determined for convergence PMP was applied to obtain a common duration of 24 hours for all the storms. Reference is made to figures and tables discussed in section 2.4 for the generalized relation. A monthly 6/24-hr ratio was interpolated from the appropriate map (figs. 2.25 to 2.27) at the location of storm rainfall. Entering table 2.7 or figure 2.20 with the 6/24-hr ratio and the duration of the rain amount gives the factor by which the rain amount needs to be adjusted to provide an estimated amount for the 24-hr duration.

c. Adjustment for maximum moisture. One of the steps in estimating PMP is to adjust observed storms to the maximum moisture potential for the storm location and date. Maximum 12-hr persisting 1000-mb (100-kPa) general-storm dew points (Schwarz and Hansen 1978) were used in this adjustment. The adjustment assumes a pseudo-adiabatic lapse rate with a saturated atmosphere and is the ratio of precipitable water for the maximum 1000-mb (100-kPa) dew point to that for the storm dew point at a location representative of the inflow moisture. A further maximization was made by allowing the maximum 12-hr persisting 1000-mb (100-kPa) dew point to be read 15 days toward the seasonal maximum.

2.2.2 Enveloping 12-hr Persisting Dew Points

Enveloping 12-hr persisting dew points have been developed and presented in HMR Nos. 36 and 43 and on a national basis in the Climatic Atlas (Environmental Science Services Administration 1968). The companion volume to the present study (Schwarz and Hansen 1978) updates the data for the Southwest and develops both general- and local-storm 12-hr maximum persisting 1000-mb (100-kPa) dew points.

2.2.3 Regional Patterns

The adjusted storm amounts in the last column of table 2.1 were plotted at their respective locations on a map (not shown). The few data points provided the lowest level of convergence PMP to be considered at these locations but were insufficient to define a regional pattern.

One approach to regional patterns was based on maximum 1-day precipitation for each month in the least-orographic regions in the Southwest. All long-record (>20 years) stations considered least-orographic within each subregion are listed in table 2.2 and are located by numbered dots in figure 2.1. Maximum monthly 1-day rains were obtained from Technical Paper No. 16 (Jennings 1952) and supplemented by recent records through 1970. Averaged maximum values, by month within each subregion, were helpful but not sufficient to define regional patterns, due primarily to the small number of data points. A further step of adjusting the data to a common elevation and for upwind barriers did not help materially.

Additional guidance for regional patterns of 1000-mb (100-kPa) convergence PMP came from analysis of moisture potential. The Climatic Atlas (Environmental Science Services Administration 1968) presents charts of maximum persisting 12-hr 1000-mb (100-kPa) dew points covering the 48 conterminuous states. These charts were used because they portray the broadscale moisture patterns influencing the Southwest. The use of revised moisture charts for the Southwest would not affect the conclusions on moisture patterns based on that Atlas. Figure 2.3 shows examples of schematic charts adapted from the January and August dew point charts from the Atlas. These schematics suggest the source of atmospheric moisture for the region. The solid lines are used to imply moisture from the Gulf of Mexico, while the dashed lines suggest moisture from Pacific Ocean sources. The change in orientation of the dashed lines between January and August reflects a change from mid-latitude storms in winter and spring to moisture surges from tropical latitudes in late summer. The dotted lines represent smoothing in the transition zone between the two moisture sources.

The moisture patterns for each of the months give guidance to the pattern of regional variation but not to magnitude of precipitation. They show that the tropical Pacific moisture source has its greatest influence over the southwest region from May through October.

The Gulf of Mexico is recognized by many researchers as a source for much of the day-to-day precipitation over the Southwest. However, such rainfall occurrences are not representative of conditions for extreme precipitation (Hansen 1975a, 1975b). Precipitation climatology studies of the Southwest by Schwarz and Hansen (1978) supports this interpretation.

2.2.4 Seasonal Variation

Clues to regional patterns of 1000-mb (100-kPa) convergence PMP for each month can also be obtained from analyses of seasonal trends in precipitation data at various locations. Therefore, the seasonal variations of the maximum 1-day precipitation for the stations in least-orographic subregions shown in figure 2.1 and listed in table 2.2 were analyzed. Seasonal charts, figures 2.4a to 2.4e, show monthly averages within each subregion by open circles, along with an eye-smoothed curve (short dashes).

In figure 2.4a to 2.4e the regionally averaged 1-day maximum precipitation curves have a summertime maximum in all five regions except northwest Nevada, which shows a summer minimum and bimodal winter and late spring maximum.

Table 2.2.--Stations within least-orographic regions for which daily precipitation was available for 20 years or more before 1970.

Station	Years of rec. thru 1970	Latitude	Longitude	Elevation ft.	Elevation (m)
Southwest Arizona					
*1. Ajo, Ariz.	66	32°22	112°52	1763	(537)
2. Buckeye, Ariz.	70	33°22	112°35	888	(271)
3. Casa Grande, Ariz.	63	32°53	111°45	1390	(424)
4. Gila Bend, Ariz.	70	32°57	112°43	737	(225)
5. Maricopa, Ariz.	59	32°57	112°00	1242	(379)
6. Phoenix, Ariz	72	33°28	112°04	1083	(330)
7. Yuma, Ariz	100	32°44	114°36	138	(42)
8. Blythe, Calif.	58	33°37	114°36	268	(82)
9. Brawley, Calif.	58	32°59	115°32	-119	(- 36)
10. Calexico, Calif.	47	32°40	115°30	3	(1)
11. Indio, Calif.	71	33°43	116°14	20	(6)
12. Iron Mt., Calif.#	22	34°08	115°08	922	(281)
Northeast Arizona					
13. Jeddito, Ariz.	35	35°46	110°08	6700	(2042)
14. Leupp, Ariz.	22	35°17	110°58	4700	(1433)
15. Tuba City, Ariz.	46	36°08	111°15	4936	(1504)
16. Winslow, Ariz.	55	35°01	110°44	4880	(1487)
17. Bluff, Utah	59	37°17	109°33	4320	(1317)
18. Green River, Utah	64	39°00	110°09	4087	(1246)
19. Hanksville, Utah	45	38°25	110°41	4456	(1358)
20. Crownpoint, N.Mex	63	35°40	108°13	6978	(2127)
21. Farmington, N. Mex.	64	36°43	108°12	5300	(1615)
Western Utah					
22. Black Rock, Utah	48	38°45	113°02	4860	(1481)
23. Deseret, Utah	77	39°18	112°38	4541	(1384)
24. Dugway, Utah#	20	40°10	113°00	4359	(1329)
25. Enterprise B.Jct., Utah#	30	37°43	113°39	5220	(1591)
26. Kelton, Utah	52	41°45	113°08	4225	(1288)
27. Lucin, Utah	45	41°22	113°50	4413	(1345)
28. Milford, Utah	49	38°25	113°01	5029	(1533)
29. Wendover, Utah	66	40°44	114°02	4239	(1292)
30. Malad, Idaho	57	42°11	112°16	4420	(1347)
Southern Nevada					
31. Beatty, Nev.	34	36°54	116°45	3314	(1010)
32. Caliente, Nev.	29	37°37	114°31	4402	(1342)
33. Goldfield, Nev.	45	37°43	117°13	5700	(1737)
34. Las Vegas, Nev.	47	36°10	115°09	2006	(611)
35. Logandale, Nev.	30	36°35	114°25	1400	(427)
36. Searchlight, Nev.	35	35°28	114°55	3540	(1079)
37. Tonopah, Nev.	44	38°04	117°14	6101	(1860)
38. Needles, Calif.	22	34°46	114°38	913	(278)
Northwest Nevada					
39. Battle Mt., Nev.	81	40°37	116°52	4528	(1380)
40. Elko, Nev.	109	40°50	115°47	5075	(1547)
41. Fallon Exp. Sta., Nev.	73	39°27	118°47	3965	(1209)
42. Lovelock, Nev.	73	40°12	118°28	3977	(1212)
43. Sand Pass, Nev.	49	40°19	119°48	3900	(1189)
44. Sulphur, Nev.	34	40°54	118°40	4044	(1233)
45. Winnemucca, Nev.	82	40°54	117°48	4314	(1316)
46. McDermitt, Nev.#	20	42°00	117°43	4427	(1349)

*Location identification number in figure 2.1.

[Station information from Technical Paper No. 16 (Jennings 1952) except when noted by # from hourly precipitation records.]

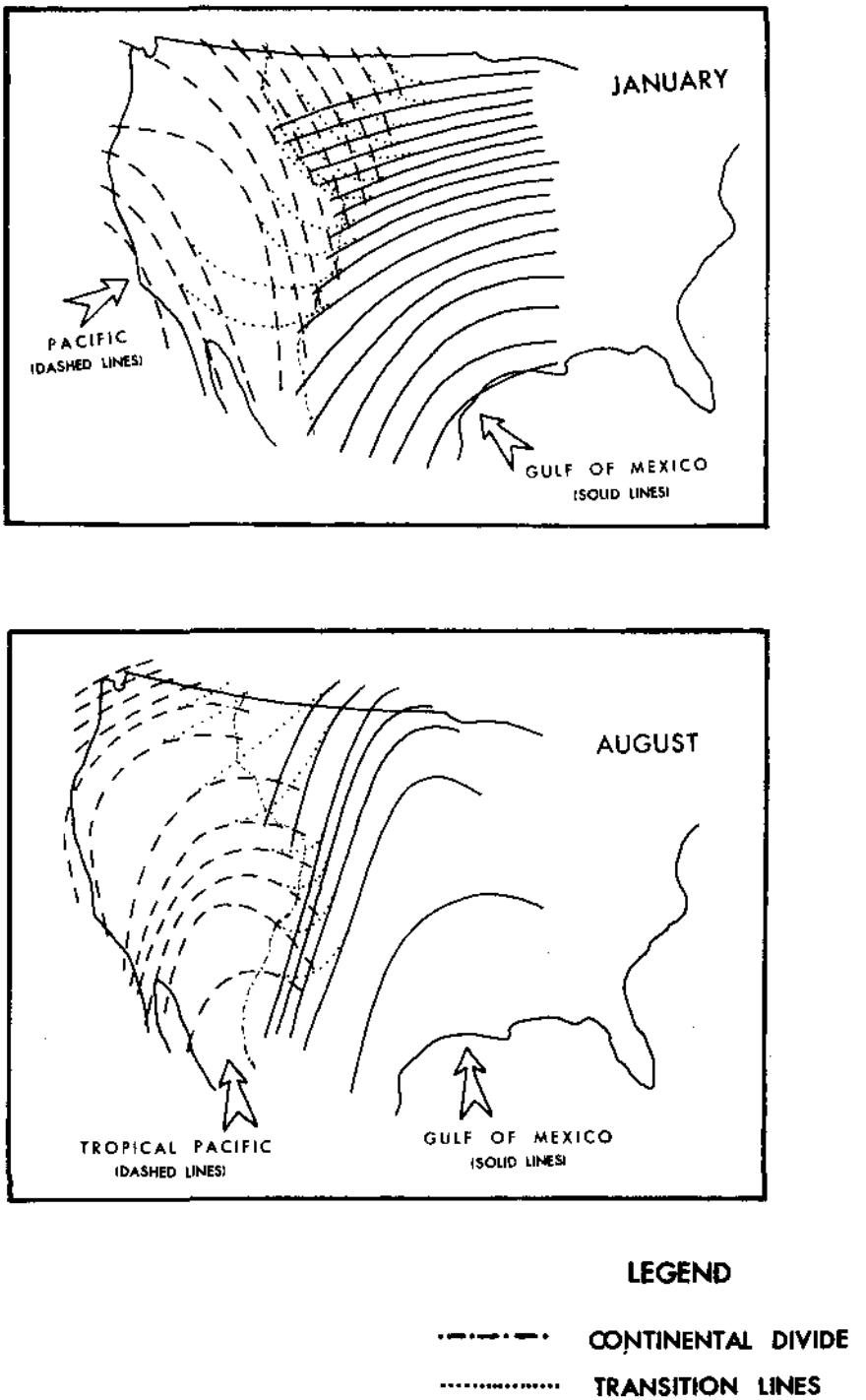

Figure 2.3.--Examples of schematic diagrams depicting moisture sources (arrows) implied by gradients of 12-hr persisting 1000-mb (100-kPa) dew points, January and August.

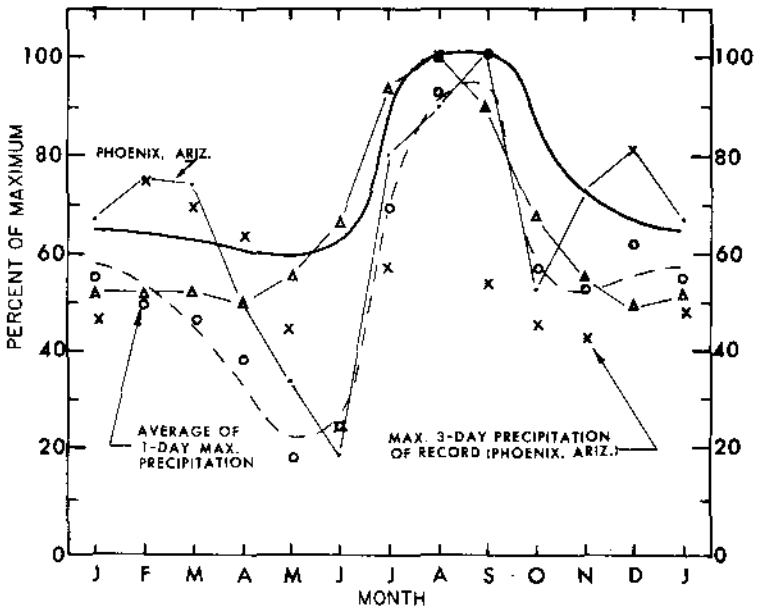

a. Southwest Arizona

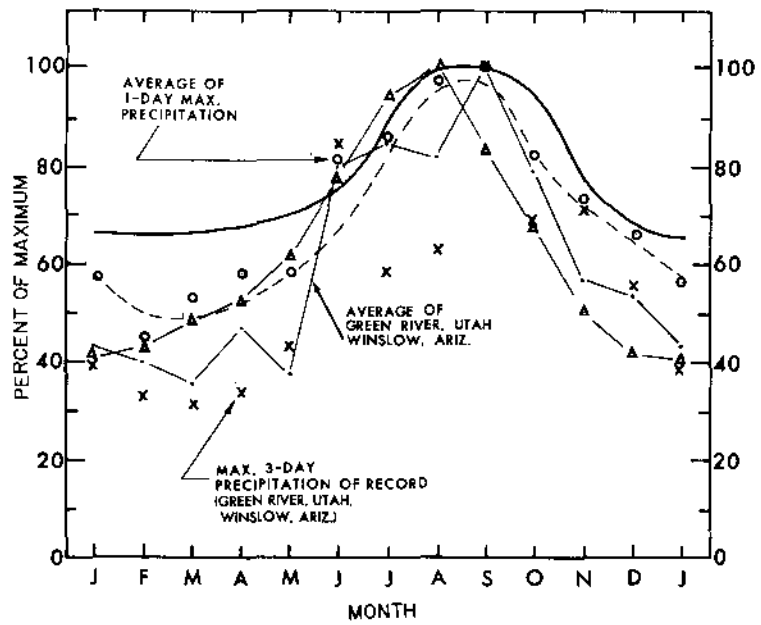

b. Northeast Arizona

▲——▲ Maximum precipitable water at subregion midpoint
– – – – – "Eye" smoothed 1-day station average (stations listed in table 2.2)
·——·—— 0.02 probability level of 3-day maximum rains
——— 1000-mb (100-kPa) convergence PMP at subregion midpoint taken from analyses in figures 2.5 to 2.16

Figure 2.4.--Seasonal variation of convergence PMP and supporting data for least-orographic subregions. All values given in percent of the maximum monthly value for that parameter.

c. Western Utah

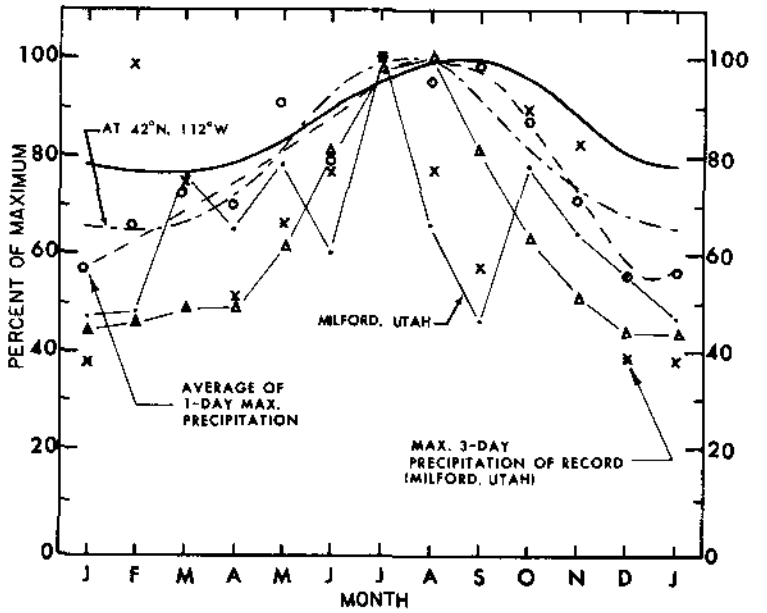

d. Southern Nevada

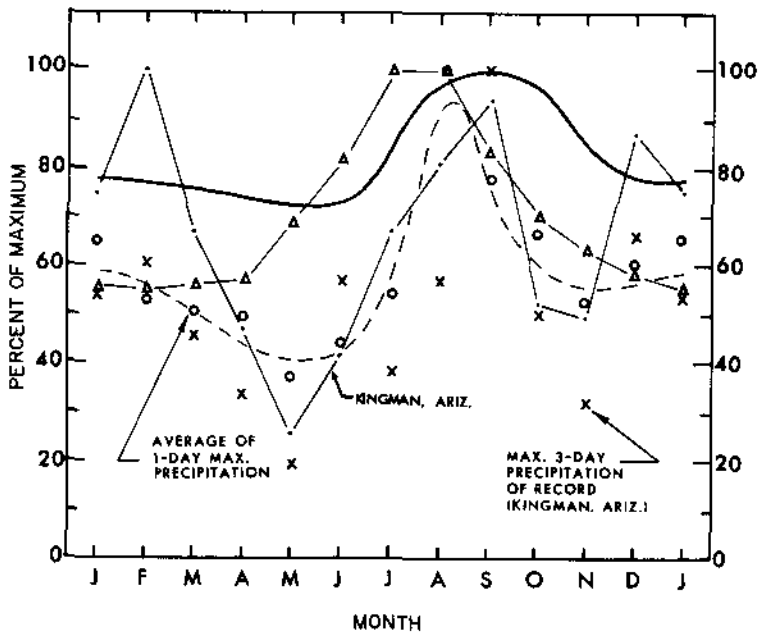

— — — — Convergence PMP (HMR No. 43)
—▲— Maximum precipitable water at subregion midpoint
— — — — "Eye" smoothed 1-day station average (stations listed in table 2.2)
•—•— 0.02 probability level of 3-day maximum rains
——— 1000-mb (100-kPa) convergence PMP at subregion midpoint taken from analyses in figures 2.5 to 2.16

Figure 2.4.--Seasonal variation of convergence PMP and supporting data for least-orographic subregions. All values given in percent of the maximum monthly value for that parameter.

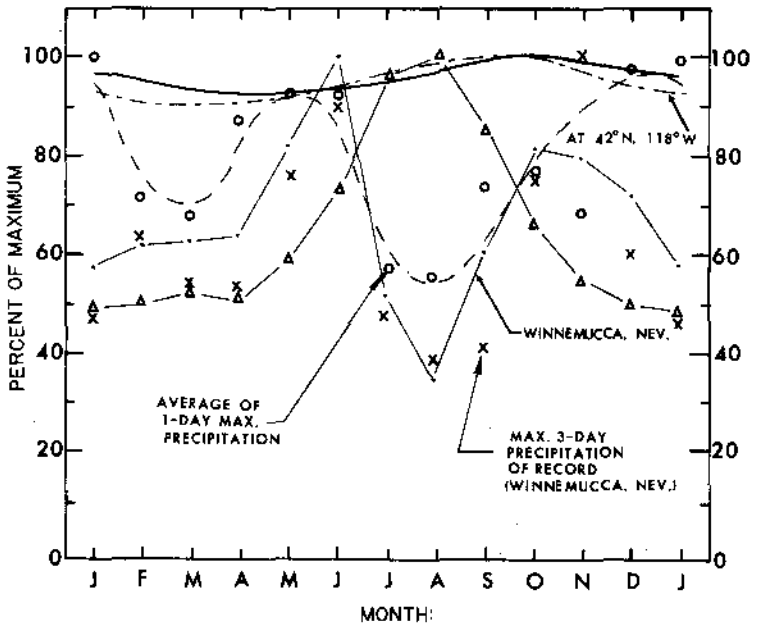

e. Northwest Nevada

- - - - Convergence PMP (HMR No. 43)
▲—▲— Maximum precipitable water at subregion midpoint
— — — — "Eye" smoothed 1-day station average (stations listed in table 2.2)
·—·— 0.02 probability level of 3-day maximum rains
——— 1000-mb (100-kPa) convergence PMP at subregion midpoint taken from analyses in figures 2.5 to 2.16

Figure 2.4.--Seasonal variation of convergence PMP and supporting data for least-orographic subregions. All values given in percent of the maximum monthly value for that parameter.

Southwest Arizona and southern Nevada show spring minimums while northeast Arizona has a late winter minimum and western Utah has a winter minimum. The 1-day maximum values from June to November very likely are influenced by local-storm rainfalls.

Another rainfall statistic considered was maximum 3 consecutive observation day precipitation. These data reduce some of the bias due to thunderstorm rainfall, particularly in summer when short-duration thunderstorms predominate. In addition to the maximum for each month, the 0.02 probability level of maximum 3 consecutive observation-day precipitation was computed for stations in each subregion. This is shown on figures 2.4a to 2.4e by dot-dashed lines. The 0.02 probability level was computed using the Fisher-Tippett type I distribution fitted by the method of Gumbel from the series of maximum monthly values for each year from approximately 50 years of record (1912-61) for one station within each subregion. Kingman, Ariz., while somewhat beyond the regional limits, was used for the southern Nevada subregion.

In figures 2.4a to e, the seasonal trends in the 1- and 3-day data are comparable with some exceptions, most notably between October and February in northwest Nevada (fig. 2.4e) in which the trends appear opposed. Some rather large differences occur for specific months as in September in figures 2.4a, c, d, and e, and February in figures 2.4a and c. All five figures show the seasonal tendency of the 0.02 probability values to generally follow the trends in the 1- and 3-day data. A large exception for one month appears in the 0.02 probability peak in February in figure 2.4d.

In additon to the maximum rainfall data, an index to moisture potential was considered for additional input to the seasonal variation problem. Potential moisture in the form of precipitable water associated with the maximum 12-hr persisting dew points was determined. The dew points were read from the analyses developed for the Southwest general storms (Schwarz and Hansen 1978) at mid-points of each subregion. These data have been entered on figures 2.4a to 2.4e in percent of maximum precipitable water amount (dash triangle curve). All five subregions show late summer maxima (July or August) with broad minimums through the winter months, extending into spring.

Figures 2.4c and 2.4e, also show seasonal curves of 24-hr 1000-mb (100-kPa) convergence PMP (alternate long-short dashes) taken from HMR No. 43 at the southern edge of the region of that report. Although HMR No. 43 covers only the months of October to June, the data were extended through the remaining months by simple extension of smoothed curves. Table 2.3 gives the smoothed values considered at these two locations.

Table 2.3.--Seasonal variations of 1000-mb (100-kPa) convergence PMP for 24 hrs, from HMR No. 43 (U. S. Weather Bureau 1966a).

Location		Jan	Feb	Mar	Apr	May	Jun	July	Aug	Sept	Oct	Nov	Dec
42°N 118°W	in.	8.60	8.45	8.37	8.46	8.50	8.70	(8.93)	(9.18)	(9.30)	9.20	9.00	8.75
(Northwest Nevada)	mm	218	215	213	215	216	221	(227)	(233)	(236)	234	229	222
42°N 112°W	in.	8.30	8.15	8.40	9.25	10.30	11.80	(12.72)	(12.80)	(11.70)	10.50	9.28	8.55
(Northern Utah)	mm	211	207	213	235	262	300	(323)	(325)	(297)	267	236	217

Values in parentheses estimated from interpolation, based on smooth seasonal distribution.

2.2.5 PMP Storm Prototypes

Another consideration before we can develop mid-month convergence PMP maps is to determine what type(s) of storm(s) is (are) likely to produce general-storm PMP in the Southwest, and the seasonal and regional variations of the general storm.

An extensive review of the meteorology of Southwestern storms is presented, with examples, in the companion volume (Schwarz and Hansen 1978). Nevertheless, brief comments are included here to establish the trend in storms that are considered representative of producing rainfall of PMP magnitude.

Through most of the Southwest, the decadent tropical cyclone is considered the PMP prototype for the period from the end of June to mid-October. Examples of record are the storms of September 1939, August 1951, and September 1970. In the southern portion of the region during the cool season, fronts and storm centers from the Pacific Ocean produce major rains. Slow-moving to stagnant frontal situations, as in December 1955 and January 1916, are examples.

The summer tropical cyclone is not likely to penetrate into the northwest or extreme northeast corners of the study area. For all-season PMP in the northwest portion, storms with more westerly moisture flows can enter the region around the north end of the Sierra Nevada range. This has led to the conclusion that northwest Nevada would have a seasonal influence more closely allied to northern California, where the October 1962 storm produced extreme rains.

The northeast corner, particularly north of the Uinta Mountains and east of the Wasatch Mountains, can be influenced by moisture flows from the east that have spilled around the northern end of the Rocky Mountains in Colorado. Although no prototype storm for this northeast corner has yet been observed, the June 1964 storm that struck the Montana Rockies is an example of the type of storm that could affect this portion of the Southwest. Thus, seasonally, the northeast corner is similar to the eastern boundary region in HMR No. 43.

Exact boundaries for the zone of influence of each type of storm have not been delineated. Rather, their influence has been incorporated in part by adjustments in the barrier elevation chart (see section 2.3) to account for the expected flows, and in part by the seasonal variations built into the convergence PMP analyses through tie-ins to peripheral studies. To understand the result and effectiveness of these methods, see the discussion in chapter 5 on checks on PMP level.

2.2.6 Development of 10-mi^2 (26-km^2) 24-hr Convergence PMP

In the development of seasonal maps of convergence PMP a number of considerations were used as guidance. Not necessarily in the order of importance, These were to:

a. Envelop all maximized values of observed rainfall in least-orographic areas without explicit transposition.

b. Recognize trends in seasonal variations established by data from least-orographic stations.

c. Recognize the potential summertime maximum precipitation represented by the seasonal variation of maximum precipitable water.

d. Fit a pattern that is in accord with tracks of extreme rain-producing storms.

e. Observe regional variations caused by influences of different prototype storms.

This formed the nucleus of the scheme for developing Southwest convergence PMP. Since the Northwest PMP report presented monthly maps of convergence PMP (except July to September), these were selected as the point of begining. The California PMP report does not provide a seasonally variable pattern of convergence PMP although values are given for October through April. Therefore, some discontinuity existed between the Northwest and the California results. Most important was the fact that the patterns of gradients between the two studies were compatible.

The procedure began by simply extending the gradient patterns of 1000-mb (100-kPa) convergence PMP from the Northwest into the Southwest. The maximized value at Indio (table 2.1) gives the limiting magnitude for the month of September at that location. The eye-smoothed 1-day data curve of figure 2.4a was used to get an initial seasonal variation of magnitude at Indio taking the September value as 100%. It was obvious that the deep minimum in spring of this seasonal curve was not in agreement with a consistent pattern of extended gradients from HMR No. 43. The Indio seasonal curve was modified by increasing the spring values to be more in line with the broad winter-spring minimum shown by the moisture curve in figure 2.4a.

From this beginning the next consideration was how to treat the west slopes of the Rocky Mountains. East of the 105th meridian HMR No. 51 (Schreiner and Riedel 1978) shows a tight gradient of PMP having a NE-SW orientation of isohyets of PMP. Because the general level of convergence PMP for the Southwest is much less than that shown by HMR No. 51, it is necessary to create a tight gradient somewhere between these two regions. PMP for the mountainous region between the Continental Divide and 105th meridian has yet to be studied in detail. We assume that much of the decrease in magnitude of PMP from HMR No. 51 will be concentrated near the Divide. Therefore, a tighter gradient was maintained along the west slopes of the Rockies than over most of the remainder of the Southwestern Region.

Considerations c, d, and e were particularly involved with interpretation of the pattern of PMP gradients during the period of summer maximum precipitation, expected to come from a decadent tropical cyclone. The influence of this PMP prototype storm through much of the region is especially important in the southern portion of the region, closest to the source of moisture, and extends from July to September. This causes the isohyets to become aligned more east-west at lower latitudes. An assumption of equal likelihood of the summer prototype general storm between July and early October is supported by monthly distributions of eastern Pacific tropical cyclones (Rosendal 1962, Serra 1971, Baum 1974). Thus a rather broad seasonal maximum in convergence PMP results through the southern portion of the Southwest.

With these considerations in mind, a preliminary set of monthly PMP maps was constructed tying magnitudes and gradients along the north to HMR No. 43, along the west to HMR No. 36, and using the Indio maximized value as a control on the magnitude in the southwest section. Pattern and magnitude in the eastern sections were controlled to a lesser extent by HMR No. 51.

Seasonal values of convergence PMP were read for mid-points of the five least-orographic subregions from these preliminary maps and compared to the 1-day, 3-day, and moisture curves shown in figures 2.4a to 2.4e. Smoothing and adjusting of the set of preliminary maps resulted in a consistent series of seasonal curves and maps.

The finalized set of 1000-mb (100-kPa) 10-mi^2 (26-km^2) 24-hr convergence PMP maps is presented in figures 2.5 to 2.16. Whereas, the initial maps began as extensions of the isohyets in HMR No. 43, the final maps after smoothing no longer maintain the direct association. For some individual months differences in magnitude of up to 1 inch exist at some border locations. The greatest differences in pattern between these two studies occur in April and November, both considered transition months in terms of synoptic storm influences.

Final mid-month convergence PMP values were read from figures 2.5 to 2.16 for the least-orographic regions and seasonal curves for these points plotted in terms of percent of the greatest of the 12 values in figures 2.4a to 2.4e (heavy solid lines) for comparison with the data. In figure 2.4a, convergence PMP preserves the summer maximum and broadens the peak, as intended, to include the summer prototype storm over the longer period. A similar remark can be made about the convergence PMP curve in figure 2.4b.

In western Utah, figure 2.4c, the convergence PMP curve peaks in September. This is a month later than the eye-smoothed 1-day rainfall curve and the curve from HMR No. 43. The PMP maximum in September results from extension beyond the data to consider the influence of late summer tropical cyclones.

The peak in convergence PMP in figure 2.4d (Southern Nevada) is noticeably later than the moisture curve and somewhat later than the 1-day data, being broadly centered about the 3-day maximum in September.

In figure 2.4e (northwest Nevada), the convergence PMP curve has a small amplitude with a broad maximum centered on October. The October maximum is in agreement with the fall prototype storm with westerly inflow in northern California.

The resulting 1000-mb (100-kPa) convergence PMP maps of figures 2.5 to 2.16 describe a set that is generally consistent with considerations listed at the beginning of this section. With the exception of western Utah and northwest Nevada the patterns show prominent summer maxima similar to maximum moisture, but tend to show much less variation from summer to winter than do the moisture curves in all five regions. The seasonal variation of the convergence PMP should be less than the variation of moisture alone since the greater efficiency of storms in the cooler season compensates to some extent for less available moisture.

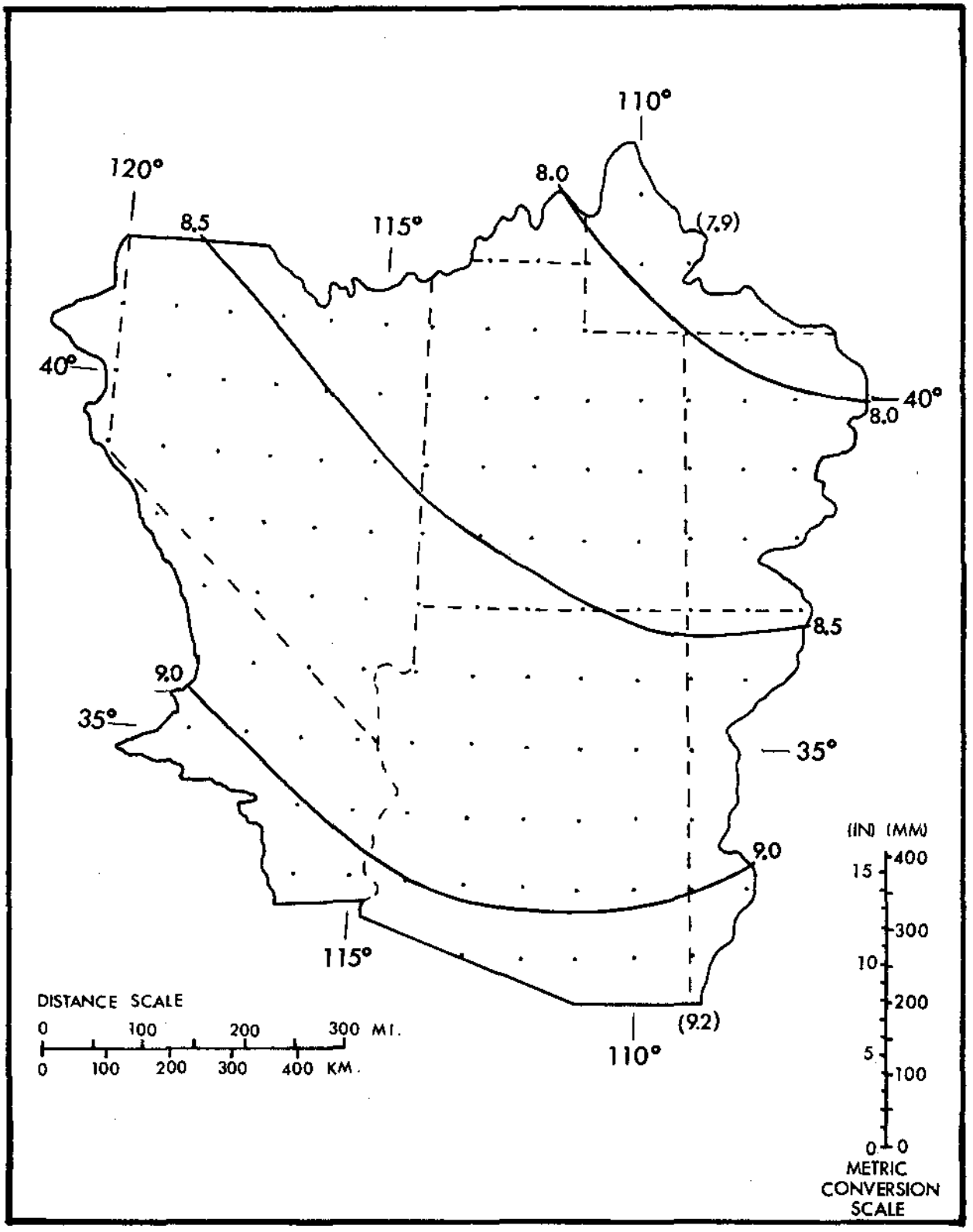

Figure 2.5.--1000-mb (100-kPa) 24-hr convergence PMP (inches) for 10 mi^2 (26 km^2) for January. Values in parentheses are limiting values and are to facilitate extrapolation beyond the indicated gradient.

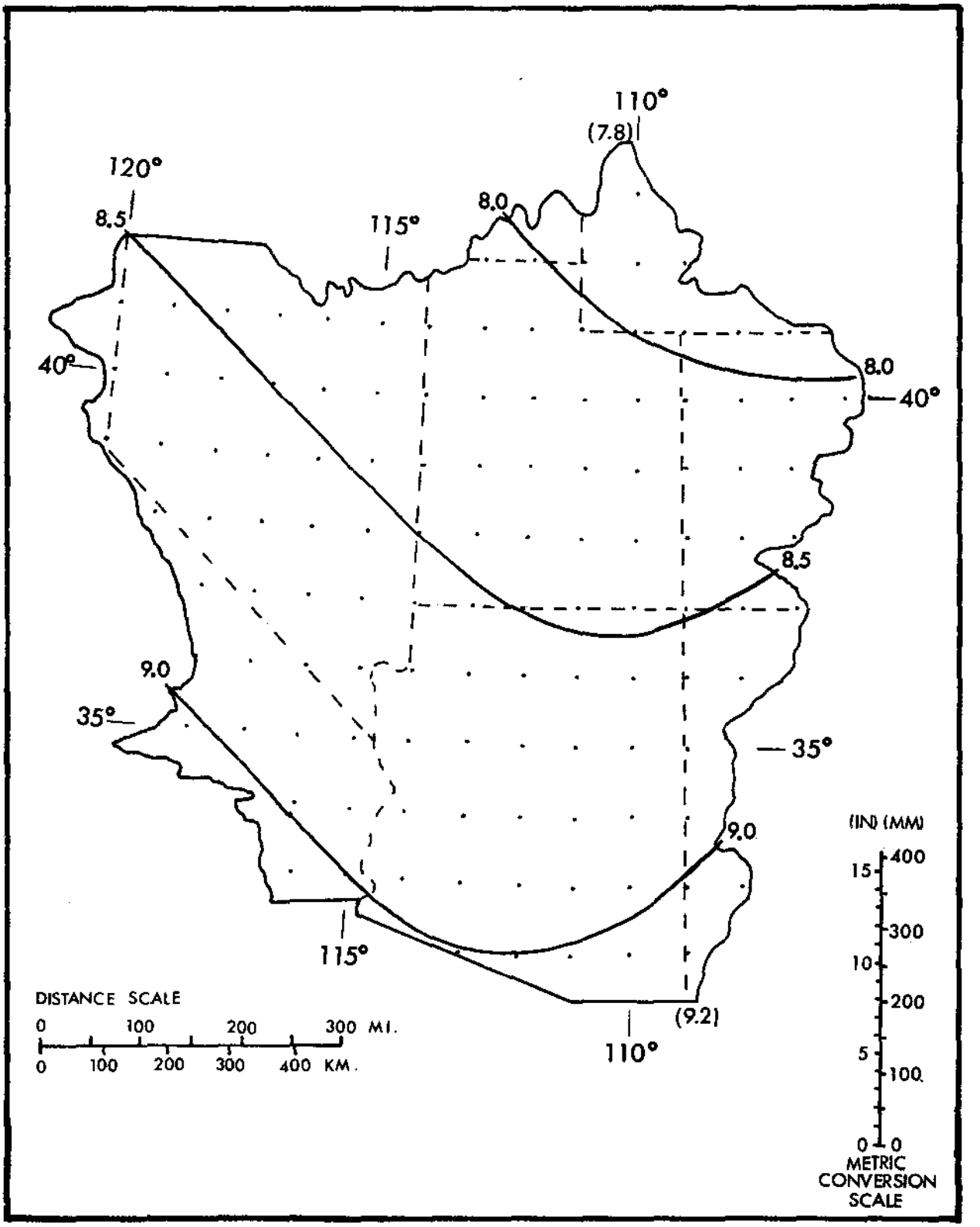

Figure 2.6.--1000-mb (100-kPa) 24-hr convergence PMP (inches) for 10 mi^2 (26 km^2) for February. Values in parentheses are limiting values and are to facilitate extrapolation beyond the indicated gradient.

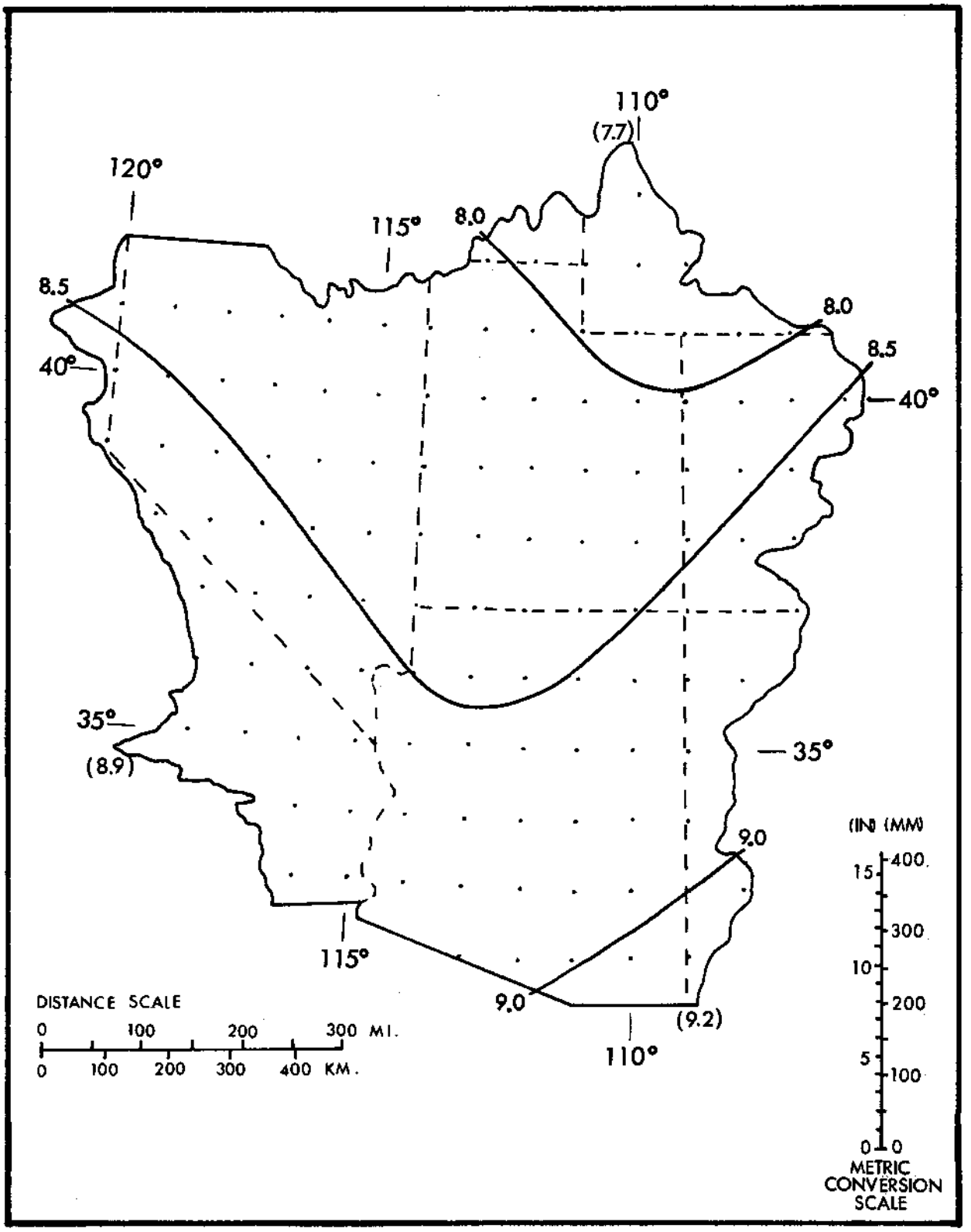

Figure 2.7.--1000-mb (100-kPa) 24-hr convergence PMP (inches) for 10 mi^2 (26 km^2) for March. Values in parentheses are limiting values and are to facilitate extrapolation beyond the indicated gradient.

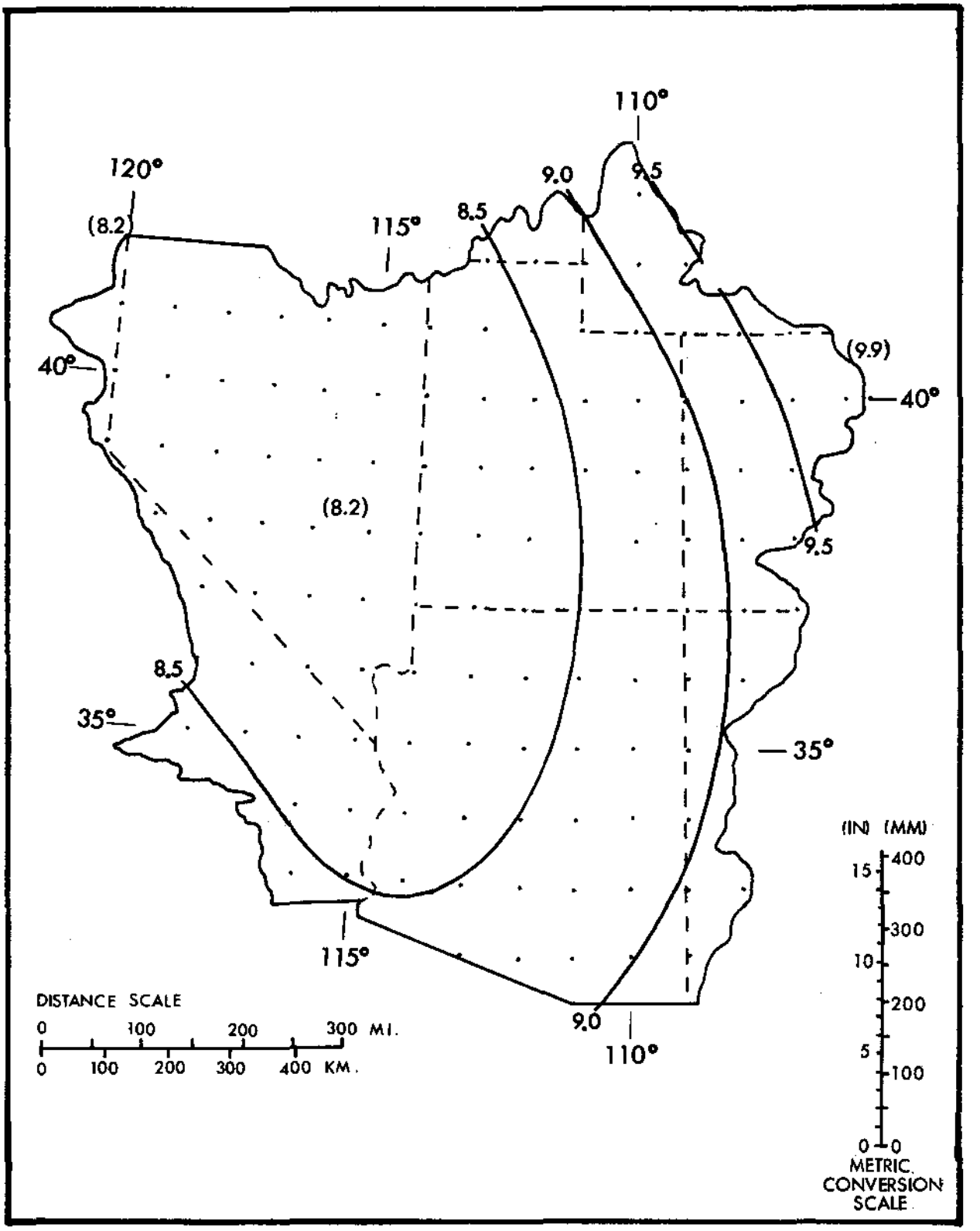

Figure 2.8.--1000-mb (100-kPa) 24-hr convergence PMP (inches) for 10 mi^2 (26 km^2) for April. Values in parentheses are limiting values and are to facilitate extrapolation beyond the indicated gradient.

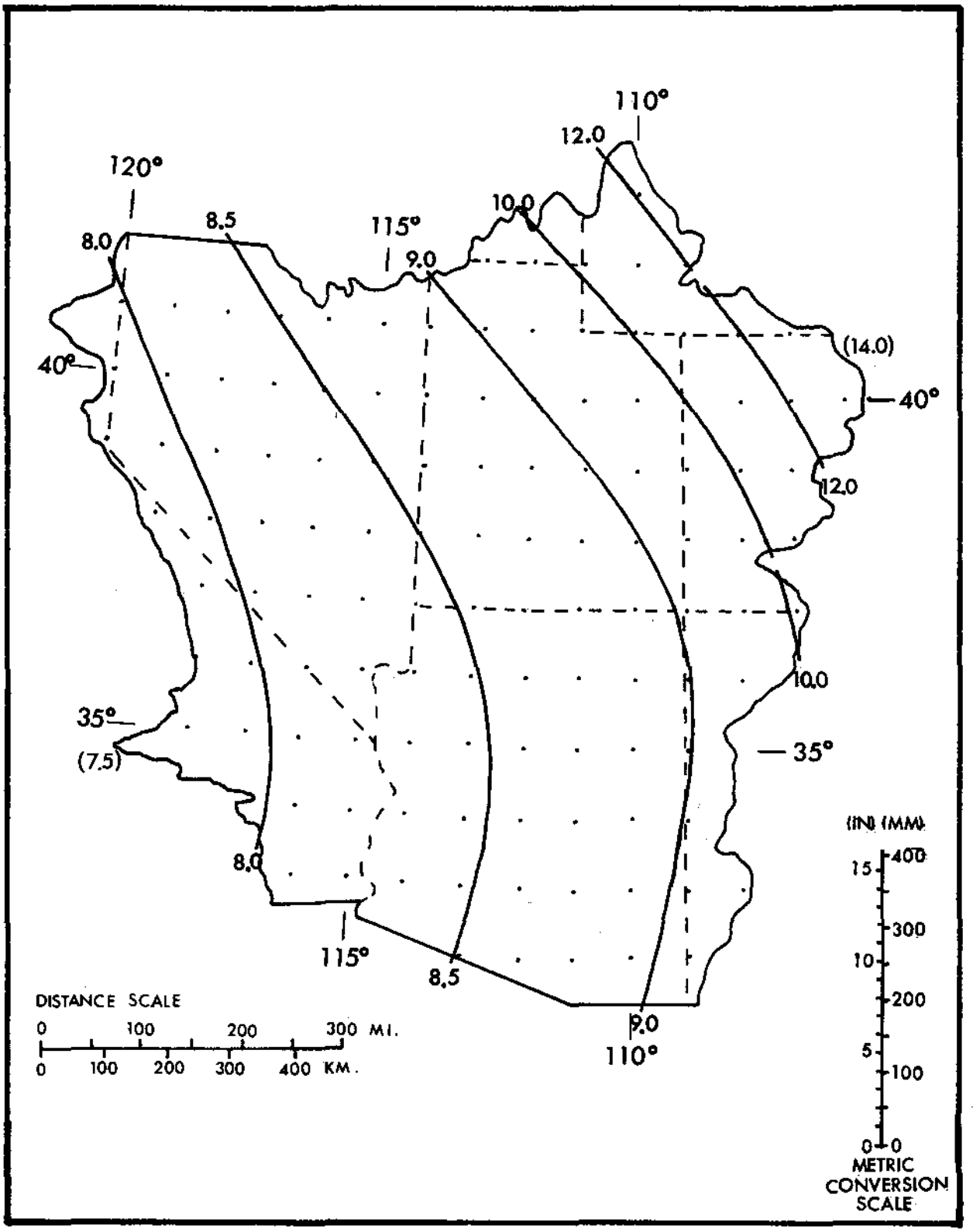

Figure 2.9.--1000-mb (100-kPa) 24-hr convergence PMP (inches) for 10 mi^2 (26 km^2) for May. Values in parentheses are limiting values and are to facilitate extrapolation beyond the indicated gradient.

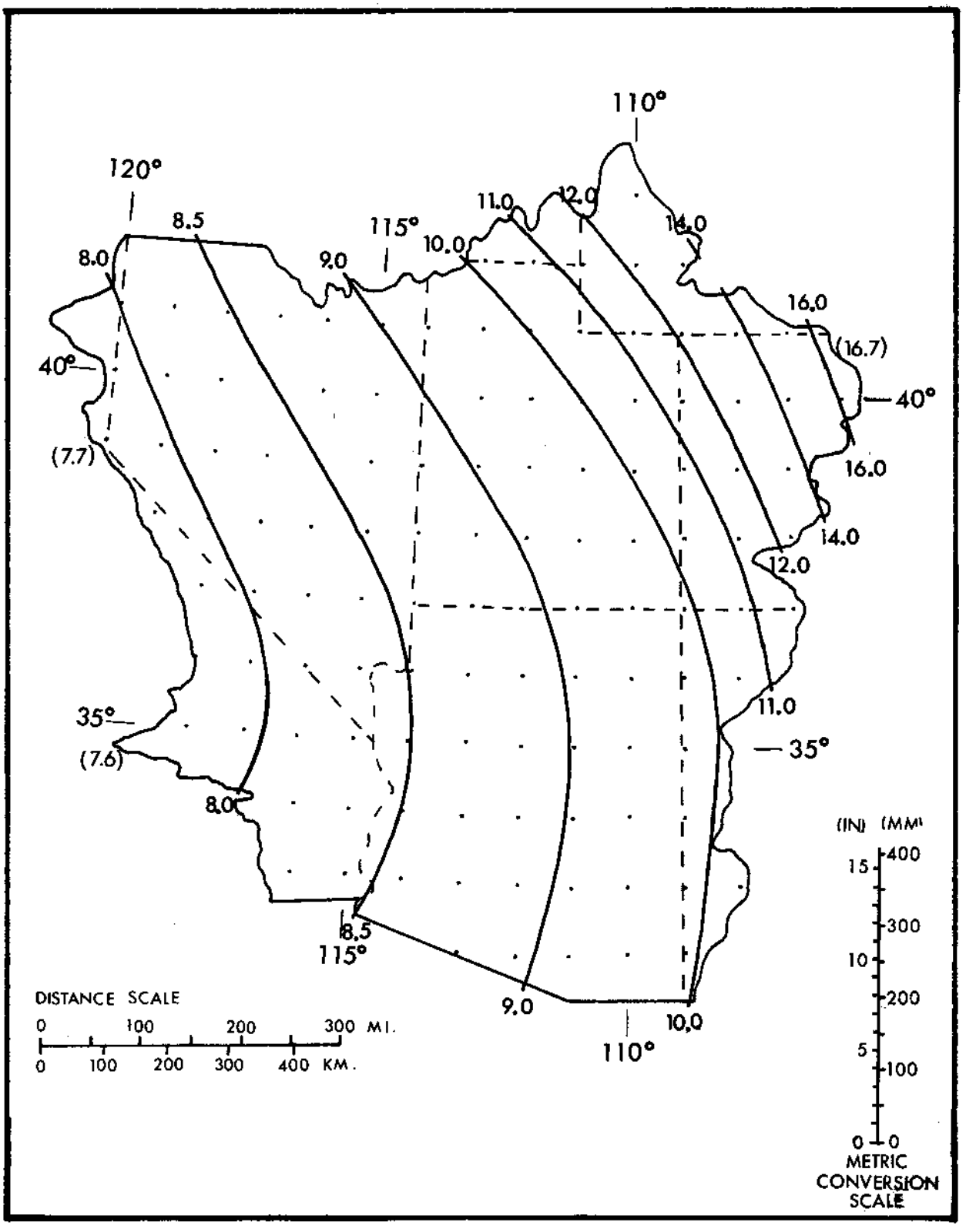

Figure 2.10.--1000-mb (100-kPa) 24-hr convergence PMP (inches) for 10 mi^2 (26 km^2) for June. Values in parentheses are limiting values and are to facilitate extrapolation beyond the indicated gradient.

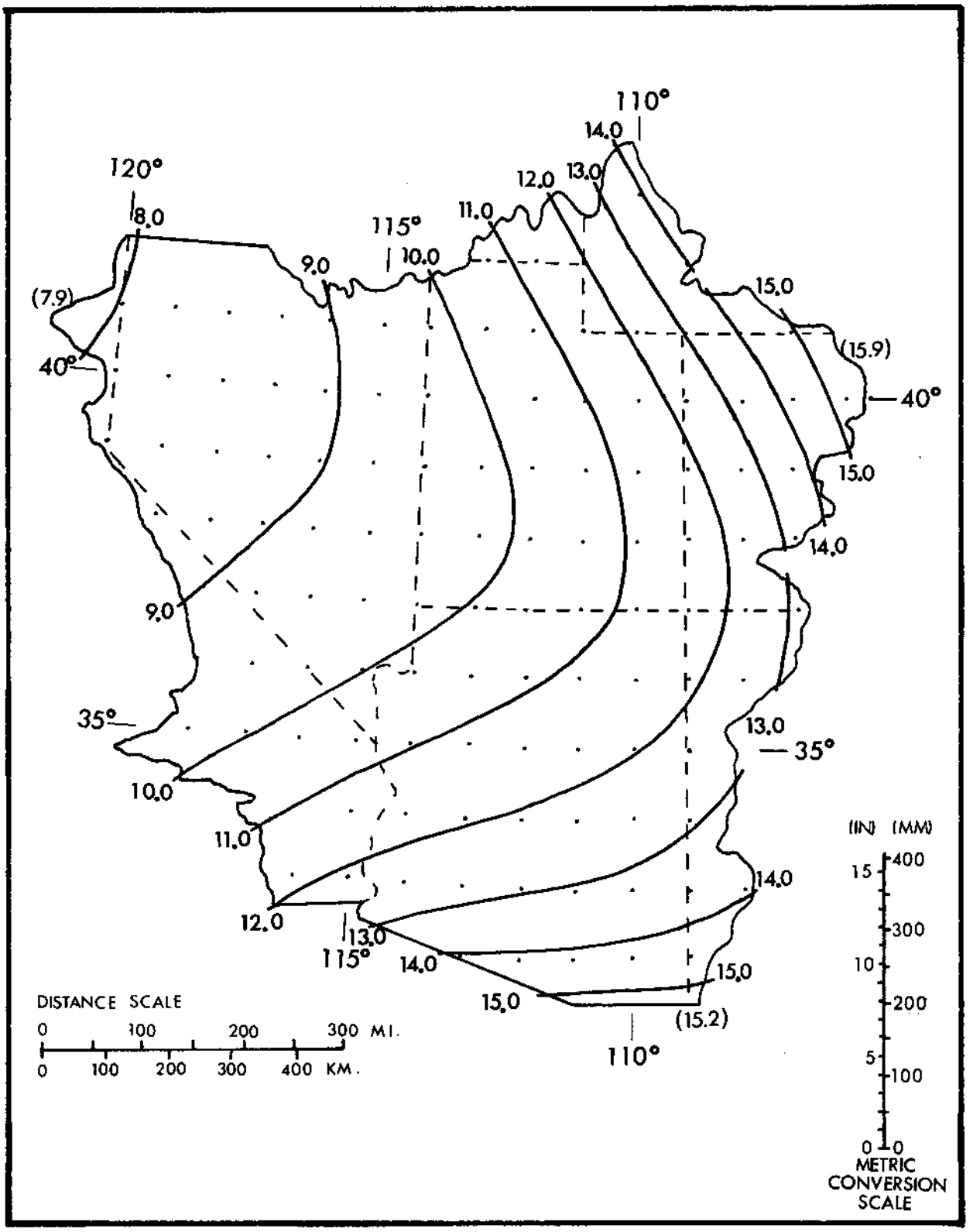

Figure 2.11.--1000-mb (100-kPa) 24-hr convergence PMP (inches) for 10 mi² (26 km²) for July. Values in parentheses are limiting values and are to facilitate extrapolation beyond the indicated gradient.

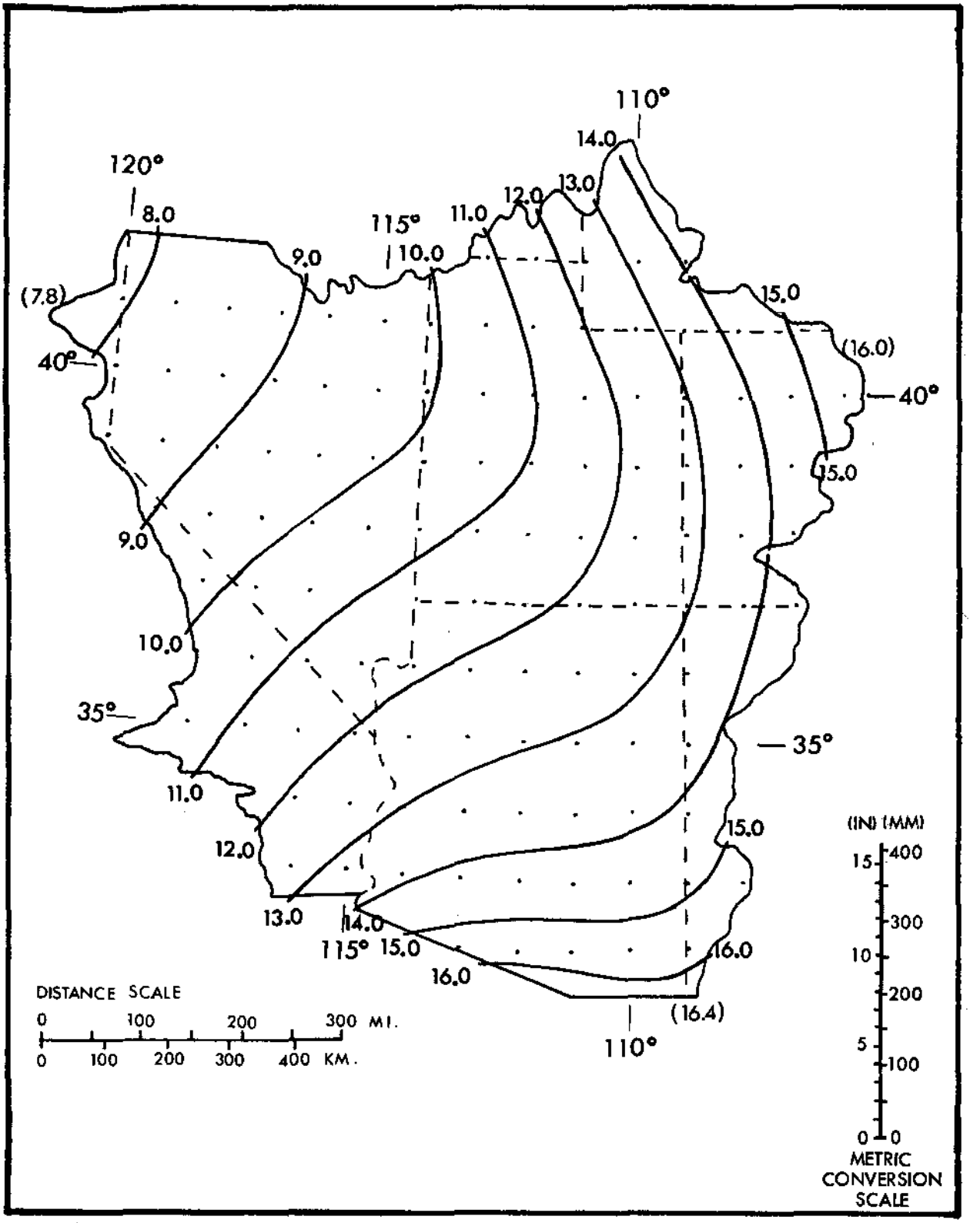

Figure 2.12.--1000-mb (100-kPa) 24-hr convergence PMP (inches) for 10 mi^2 (26 km^2) for August. Values in parentheses are limiting values and are to facilitate extrapolation beyond the indicated gradient.

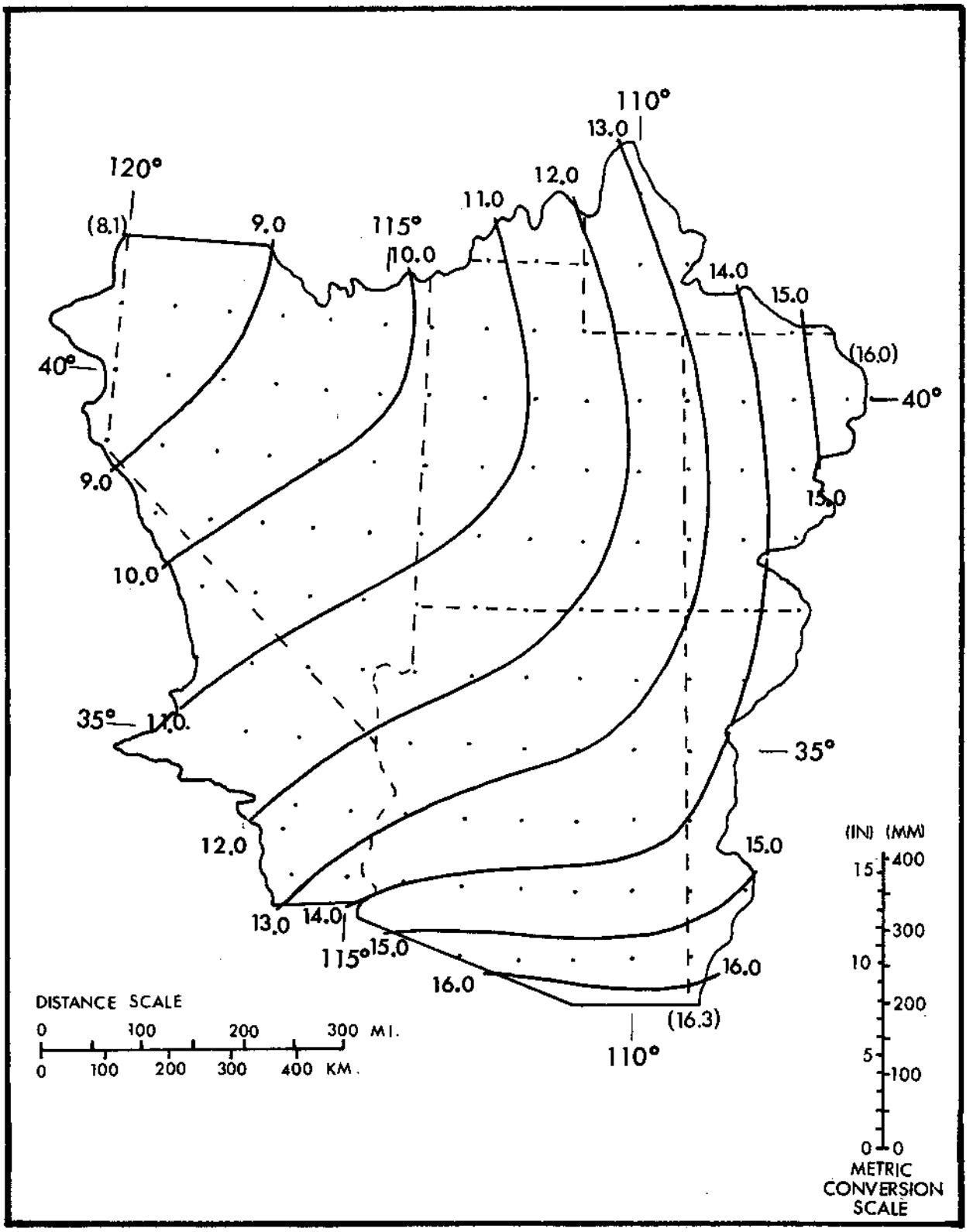

Figure 2.13.--1000-mb (100-kPa) 24-hr convergence PMP (inches) for 10 mi^2 (26 km^2) for September. Values in parentheses are limiting values and are to facilitate extrapolation beyond the indicated gradient.

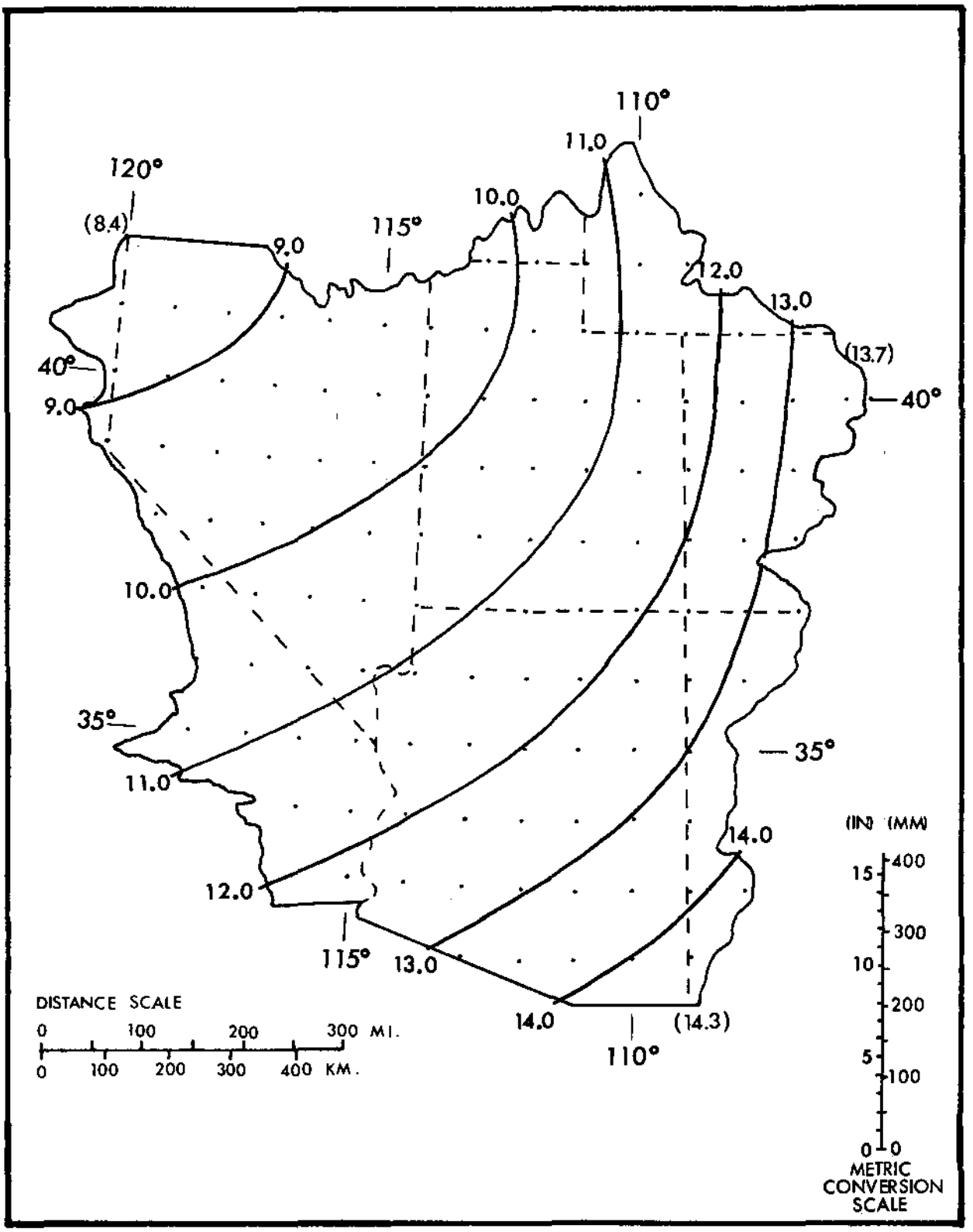

Figure 2.14.--1000-mb (100-kPa) 24-hr convergence PMP (inches) for 10 mi^2 (26 km^2) for October. Values in parentheses are limiting values and are to facilitate extrapolation beyond the indicated gradient.

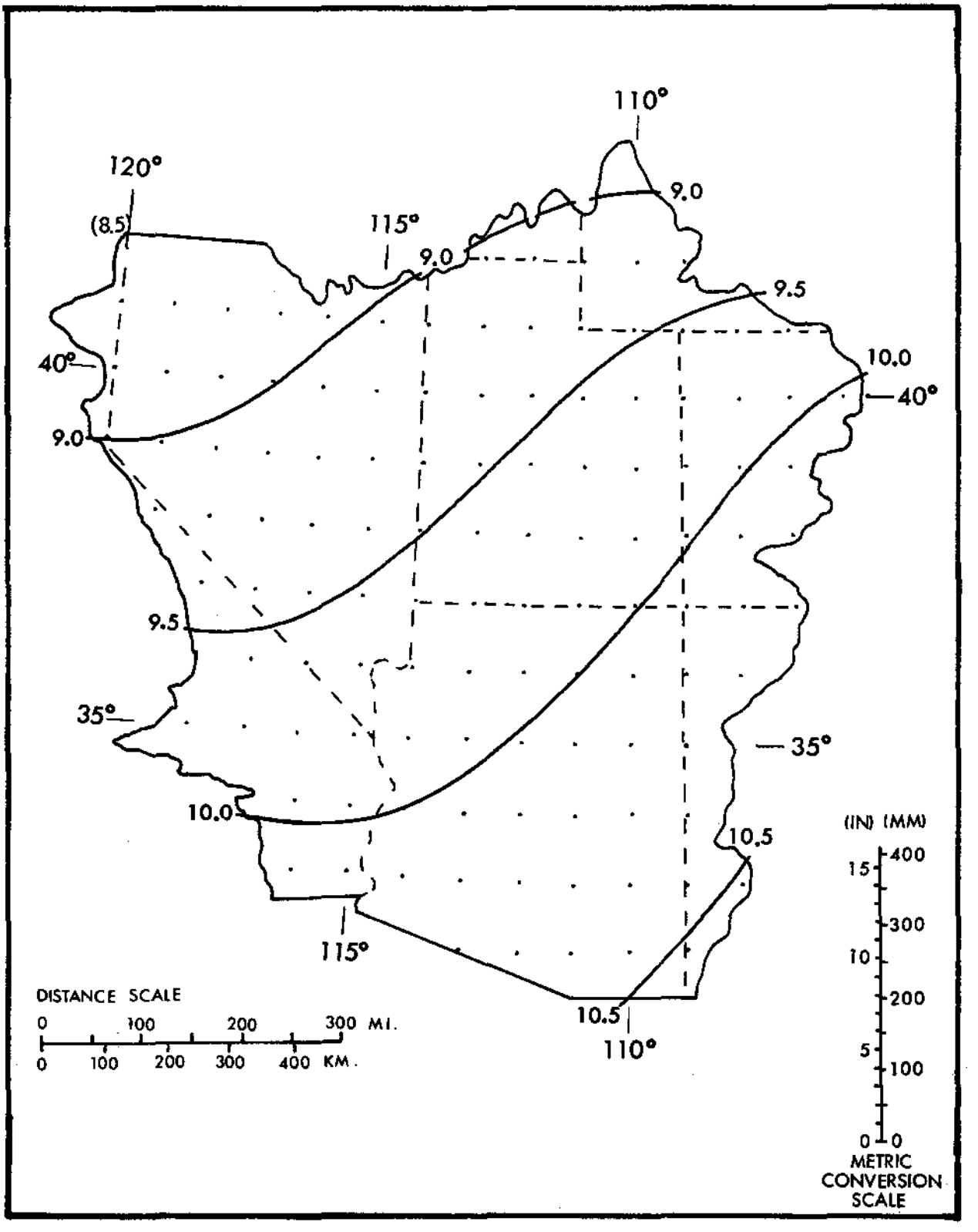

Figure 2.15.--1000-mb (100-kPa) 24-hr convergence PMP (inches) for 10 mi^2 (26 km^2) for November. Values in parentheses are limiting values and are to facilitate extrapolation beyond the indicated gradient.

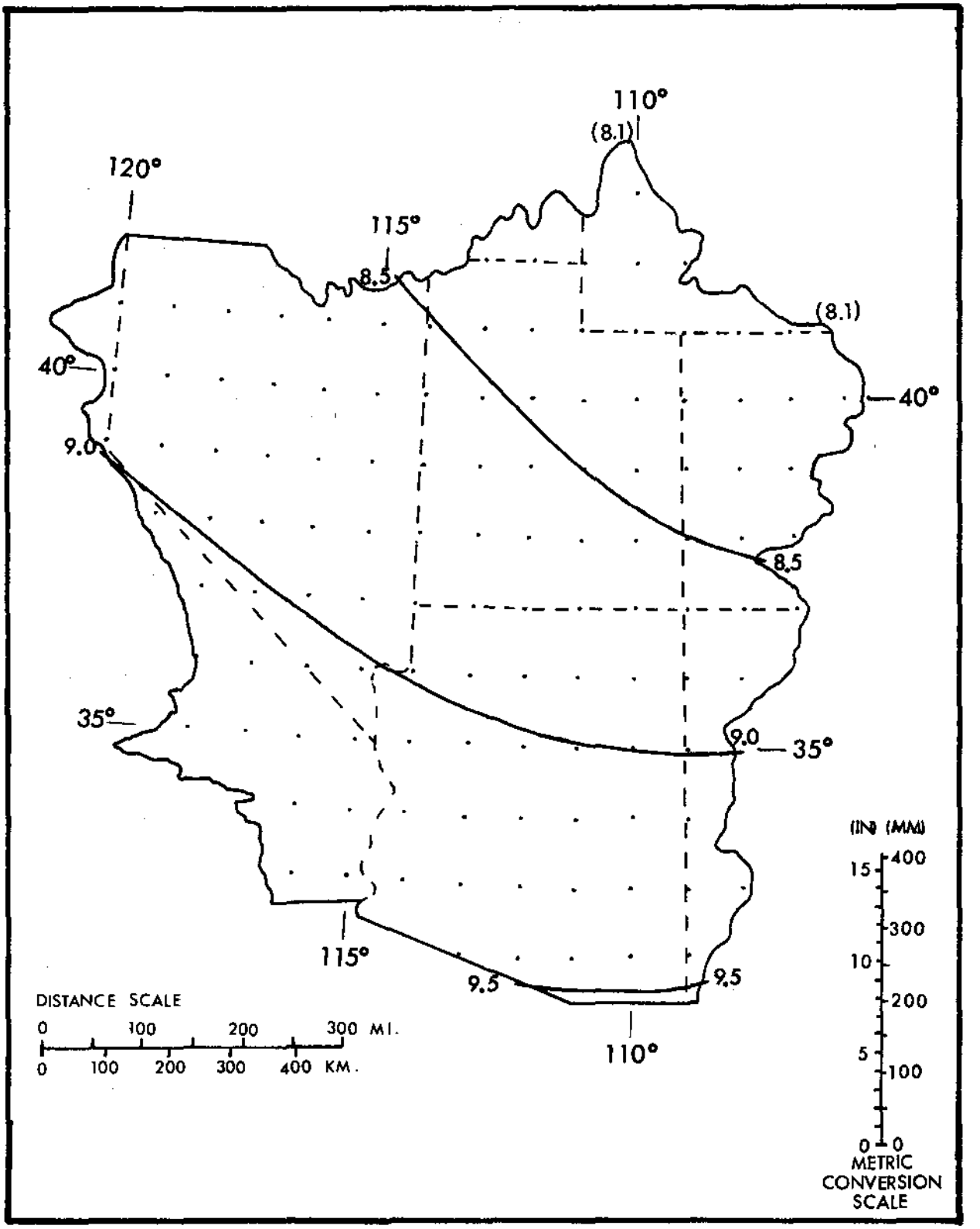

Figure 2.16.--1000-mb (100-kPa) 24-hr convergence PMP (inches) for 10 mi^2 (26 km^2) for December. Values in parentheses are limiting values and are to facilitate extrapolation beyond the indicated gradient.